Addis Ababa University
College of Natural and Computational Sciences
School of Earth Sciences

APPLICATIONS OF INTEGRATED GEOPHYSICAL TECHNIQUES TO MAP SUBSURFACE STRUCTURES, CONTRIBUTING TO GROUND WATER FLOW IN THE ZIWAY – LANGANO CORRIDOR, CENTRAL MAIN ETHIOPIAN RIFT.

By: MESFIN TADESSE

A Thesis Submitted To School of Earth Science of Addis Ababa University in Partial Fulfillment of The Requirements for the Degree of Master of Science in Exploration Geophysics.

June 2017

Addis Ababa University
College of Natural and Computational Sciences
School of Earth Sciences

APPLICATIONS OF INTEGRATED GEOPHYSICAL TECHNIQUES TO MAP SUBSURFACE STRUCTURES, CONTRIBUTING TO GROUND WATER FLOW IN THE ZIWAY – LANGANO CORRIDOR, CENTRAL MAIN ETHIOPIAN RIFT.

By: MESFIN TADESSE

Approved by

Dr Balemual Atnafu	Signature
Chairman, Department of Earth Science	
Dr Abera Alemu	Signature
Advisor	
Professor Tilahun Mamo	Signature
Examiner	
Dr Bekele Abebe	Signature
Examiner	

June2017

DECLARATION

I, the undersigned, hereby declare that the thesis entitled with **"APPLICATIONS OF INTEGRATED GEOPHYSICAL TECHNIQUES TO MAP SUBSURFACE STRUCTURES CONTRIBUTING TO GROUND WATER FLOW IN THE ZIWAY – LANGANO CORRIDOR, CENTRAL MAIN ETHIOPIAN RIFT"** is my original work carried out under the supervision of Dr. Abera Alemu and has not presented to any university or institution for the award of any degree or diploma program and all sources of materials used for the thesis are duly acknowledged.

Name of the candidate	Signature	Date
Mesfin Tadesse	_____	

This is to certify that the above declaration made by the candidate is correct to the best of my knowledge and it has been submitted for examination with my approval as university advisors.

	Signature	Date
Dr. Abera Alemu	_____	_____
(Advisor)		

ABSTRACT

The aim of this MSc thesis is to evaluate subsurface structural influences on groundwater flow in the Ziway - Langano Corridor area located in the central main Ethiopian rift using integrated geophysical methods which include gravity and magnetic method. The study is deemed to be an essential resource in evaluating the subsurface geologic structures. The surface geology of the study area ranges in composition from volcanic rocks of rhyolite, pyroclastic, obsidian, and ignimbrite rocks, to sedimentary rocks of lacustrine sediment and alluvial deposits. It is determined that the tectonic setting and rock types of an area are important in establishing the distribution of the groundwater flow.

Existence of subsurface structures which include faults, fractures, and veins have been investigated in the Ziway – Langano Corridor using horizontal gradient gravity map and tilt derivative magnetic map compiled for the study area. These geophysical investigation results have identified subsurface geologic structures which are responsible for the flow of groundwater from Lake Ziway towards Lake Langano.

In addition to this, field observations made during the magnetic survey have confirmed the flow of ground water from Lake Ziway towards Lake langano. This conclusion is also confirmed by the existence of hot springs at the northern shore of Lake Langano which is missing at the southern shore of Lake Ziway.

This work has shown that there are no east west structures that favor the flow of groundwater. Hence, the direction of groundwater flow in the study area takes place from Lake Ziway towards Lake Langano being controlled by the N-S and NE-SW oriented faults and fractures mapped in the Ziway – Langano corridor.

ACKNOWLEDGEMENT

I would like to express my sincere gratitude to Assosa University for giving me the opportunity to study my MSc in Addis Ababa University.

Above all, I like to express my heartfelt gratitude and appreciation to my Advisor, Doctor Abera Alemu**;** without his scientific advice and guidance, constructive suggestions and all way round support**;** it would have been impossible to start and complete this work.

I am grateful to the School of Earth Sciences of the Addis Ababa University for allowing me all facilities to carry out my field work.

I am thankful to Yemane Kelemewerk, and Yonathan Kerkebo for their constructive comments and suggestions.

This work would have not been successful without field data collection in Ziway-Langano Corridor of CMER. Therefore, I would like to thank Hailemichael Kebede and Tsegaye G/medhin for their supports both in the field and in the office, all members of MSc Geophysics Graduate student are greatly acknowledged for their encouragement and genuine cooperation.

I gratefully acknowledge my mother, Kiros Mekonnen and my father Tadesse Wolde who wishes all the best for me and all my brothers, especially Abebaw Tadesse, Mulugeta Tadesse and my sister Achewach Tadesse.

I wish to express my sincer gratitude to my best friends Alem Teshome, Rahmetela and Mubarek Diriba who continuously provided me important suggestion and encouragement.

I am most thankful to all my Neighbors specially Joseph Mulalem and his wife Chachu,

Finally, I would like to acknowledge our driver Thomas Dagnaw and everybody, who made it possible for me to complete this work.

TABLE OF CONTENTS

LIST OF FIGURES

ACRONYMS

AL= Aluto

AT= Adami-Tulu

CMER= Central main Ethiopian rift

GPS= Global positioning system

GSE= Geological survey of Ethiopia

IGRF=International geomagnetic reference field

Km= Kilo meter

LL= Lake Langano

LZ= Lake Ziway

M= meter

MASL= above mean sea level

MER= Main Ethiopian rift

mG= miligal

NNW= North-North West

NT= nano tesla

NW= North West

SSW= South-South West

SW= southwest

TFMAM= Total field magnetic anomaly map

CHAPTER ONE
1.0 Introduction
1.1 Backgrounds

Geophysical surveys have long been utilized by the mining and petroleum industries for several decades and basically used to determine, indirectly, the extent and nature of the subsurface geologic materials. With further development, geophysical techniques have found applications in wider areas of earth sciences addressing engineering geology, hydrogeology and environmental issues, among others.

This work deals with the application of geophysical techniques for subsurface structure studies to assess and map subsurface structures which control groundwater flow and their spatial distribution. Groundwater is simply water that occurs in the ground, in the pore spaces between mineral grains or in weathering, cracks and fractures in the rock.

In this study, primary and secondary data were collected, reviewed, analyzed and interpreted. Acquiring the secondary data includes collection of previous geophysical data including Gravity data, Topographic and Geological map relevant to the study area. The primary data comprises collection of magnetic data.

The present research is important for understanding the factors that influence the distribution and flow of groundwater. The study area is located in the Central Main Ethiopian rift (CMER). The area ranges in elevation between 2150 and 1500 m above sea level. The area is bounded between $7^0$45'N-8^0 0'N latitude and $38^0$30'E- $39^0$00'E longitude.

In the present study, gravity and magnetic data have been compiled, processed and interpreted to examine the subsurface structures and groundwater flow in the Ziway - Langano Corridor. Further, based on the results of gravity and magnetic anomaly maps, this work attempts to describe the tectonic and geologic implications of the study area.

1.2 DESCRIPTION OF THE STUDY AREA

1.2.1 Location and accessibility

The study area is located about 190km south east of Addis Ababa, In the Central MER. The study area is situated within the Lakes District region, between Lake Ziway to the north and Lake Langano to the south and forming some sort of corridor between the two lakes. Meki, Kator and Bulbla rivers are the major rivers which flow to Lake Ziway and langano. The study area cover an area of approximately 1800 square km. Geographically the study area is bounded between$7^0$45'N-8^0 0'N latitude and $38^0$30'E- 39^0 00'E latitude. In addition, there are several dry-weather farm roads crossing the area. The study area (Ziway-Langano corridor) can be accessed through two roads passing from Adami tulu to the Aluto geothermal to Lake Langano, passing through the Aluto geothermal base camp and it joins again the asphalted road at Bulbula.

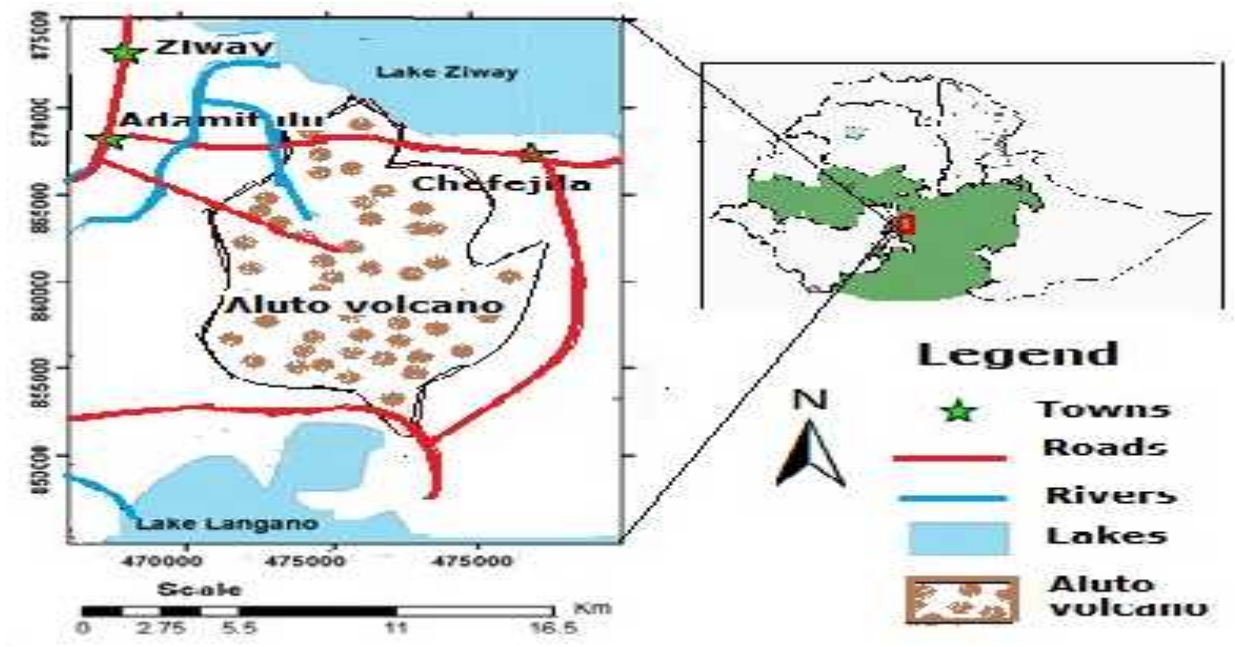

Figure 1.1 Location map of the study area

1.2.2 Physiography

The Ethiopian sector of the East African Rift system extends for more than 1000 km in a NE-SW to N-S direction from the Afar depression, at Red Sea-Gulf of Aden junction, southwards to the Turkana depression. The MER which estimated to be about 80 Km wide, separates the uplifted Somalia and Ethiopian plateau and these plateaus rises more than 2000m above mean sea level. The

rift floor increases in elevation from the Turkana depression up to the main watershed between the Meki and Awash rivers north of Lake Ziway. To the north direction the elevation of rift floor decreases as we move to the Afar depression.

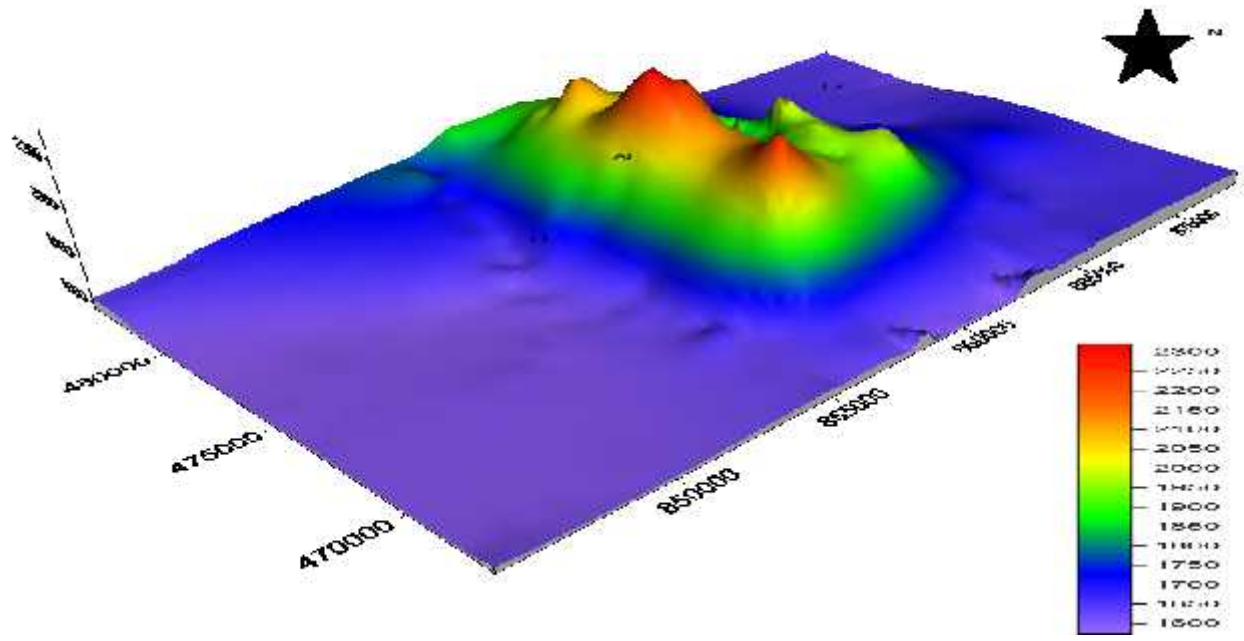

Figure 1.2 Physiographic map of the study area

1.3 Climate and vegetation cover

The Ziway-Langano Corridor appears to be a prominent topographic feature relative to the surrounding flat lands and the lake levels of Ziway (1685 m.a.s.l) and Langano (1535 m.a.s.l). The study area is characterized by warm to cool, semi-humid zone, where the annual rainfall is more than 1000mm and it is a semi-humid to arid zone. Vegetation in the floor of the rift is dominated by the spiny acacia trees and some short bushes. The top of Aluto, in particular the obsidian flows and domes are covered by denser vegetation consisting of a variety of trees and bushes.

1.4 STATEMENT OF THE PROBLEM

Geographically the study area is bounded between 7^0 45'N-8 ^{0} 0'N and 38 ^{0} 30'E- 39 ^{0} 00'E. Previously different Hydro-geological, structural and geophysical investigations were carried out in the central Main Ethiopian Rift including the study area. The previous works were not carried out for ground water investigation using integrated geophysical technique. Therefore there is still an

adequate problem for investigating the relation between subsurface structure and ground water flow in the study area. Hence a detailed study using Geophysical (Gravity and Magnetic) methods to map and characterize the subsurface structure contributing for groundwater flow in the study area will be attempted in this work.

1.5 BASIC RESEARCH QUESTIONS AND HYPOTHESIS

1.5.1 BASIC RESEARCH QUESTIONS

What are the significant geologic structures that are important for ground water flow, occurrence and storage?

1.5.2 RESEARCH HYPOTHESIS

Is there any relationship between the presence of geologic structures and the ground water flow in the study area?

1.6 Objectives of the study

1.6.1 General objective

The general objective of the study is to map subsurface structures that control the movement of groundwater along the Ziway - Langano corridor using integrated geophysical data.

1.6.2 Specific objective

The specific objective of this work is to

- Acquire new magnetic data in an attempt to fill the missing magnetic data coverage in the study area.
- Compile the total magnetic field anomaly map and its derivative maps of the study area.
- Compile the Bouguer gravity anomaly map and its derivative maps of the study area.
- Translate geophysical anomalies revealed by the compiled maps into geologic and tectonic structures of the study area.
- Map locations and estimate depths of the geologic structures that control groundwater flow in the study area.

1.7 Assumption of the Research

In this research, it is assumed that with very limited geological and hydro-geological information, the integrated use of systematically selected and affordable geophysical methods can help to understand the geological structures which control the movement and storage of groundwater. It is further expected that the geophysical surveys will provide valuable information about the subsurface structures contributing for groundwater flow.

1.8 Limitation of the research

The research has the following limitations

1. This research is aimed at contributing towards understanding the subsurface situation of the area and cannot be taken as a sole and independent methodology. It is readily established that geophysical methods are more effective when they are used with a good understanding of the geology and hydro-geological situations of the area to the extent possible. Therefore, it is not the aim of this research to claim the methodology developed in the research is stand alone.
2. The research involves only the use of commercially available instruments and software packages. There will not be any development of new instruments and software

1.9 Expected out put

This work attempts to;

- Map locations of the major subsurface geologic structures which favor the flow of groundwater in the study area.

1.10 Previous geophysical works

Most of the gravity surveys carried out in the MER is regional in scale (e.g. Hunegnaw, 1989; Alemu, 1992). These regional surveys were conducted with the objective of investigating the crustal structure of the MER.

Several gravity investigations have been made in the central MER which consists of the present study area on a semi-regional and local scale (eg. Searl and Gouin, 1972; Alemu, 1983; Ayele, 2001; Saibi, 2012). The local gravity investigations were constrained by electrical resistivity data for the assessment of the geothermal potential associated with the Aluto and Corbetti volcanoes located in the central MER. The semi-regional gravity surveys were conducted with the objective of investigating the crustal structure and the subsurface geological and structural conditions beneath the central MER.

Gravity and magnetic investigations have been made in the central MER on a semi-regional and local scale (eg.Bekele et al., 2011; Berhane, 2015: Kelemework, 2016) for geothermal exploration and investigating the crustal structure including the subsurface geological and structural conditions in the central MER.

Generally, all the previous geophysical investigations did not consider application of the geophysical methods considered (gravity and magnetic) for groundwater flow investigations. However, the current study introduces a new interpretational approach using the new and the existing gravity and magnetic data to fulfill the cited objectives of this work.

1.11 METHODLOGY

It starts with the planning stage of the research that was done by collecting all available relevant data and organizing them systematically so that a clear understanding of the problems of the area and the expected challenges can be acquired. The selection of appropriate methods was decided based on the objective of this work with due consideration of the available instruments and software packages.

1.11.1Survey Planning

Planning of the geophysical data acquisition started with the collection of all available previous information about Ziway – Langano Corridor. This was mainly found from different institutions like Ethiopian Geological Survey, Ethiopian mapping agency, Federal Mines and Water Resources. This information includes:

• Geological Map with a scale of 1:50,000

• Hydro-geological map with a scale of 1:25,000

• Topographic map of Ziway - Langano corridor at a scale of 1: 50,000

The next step in the planning process was to select profile lines and points of survey which can help to satisfy the objective of understanding the subsurface situation of the research area that controls the storage and movement of groundwater.

1.11.2. Selection of geophysical methods

All surface geophysical methods measure some physical properties of subsurface materials. Selection of the appropriate geophysical method is determined by the specific physical property of a hydrologic unit or by the differences between adjacent units. Typical physical properties measured are density and sucessptibility. Knowledge of the physical properties of a subsurface material is critical for the successful application of surface geophysical methods. Therefore, the geophysical methods used in this survey were selected based on the prominent physical characteristics of the subsurface geological structures that control the movement and storage of ground water. The approach developed in this research makes use of the different combinations of appropriately selected geophysical methods to complement the limited geological and hydrological information available. To understand the subsurface geophysical properties of the geological formations using a different kind of physical characteristics, a Gravity and magnetic survey was carried out in the Ziway – Langano corridor.

1.11.3. Selection of geophysical survey sites

Selection of the geophysical survey sites is based on different factors such as geological structures, hydro geological information and accessibility for an efficient and effective survey results

1.12 Materials

The first step in every research is to identify the available materials and data needed to solve the problem formulated/identified. Therefore, for the present study the following materials and software have been utilized.

❖Topographic map with a scale of 1:50,000 and Brunton compass were used during field survey
❖Several geological map have been reviewed to know the surface distribution of litho-logical and structural features

❖Google earth online to help assessment of the area before going to the field

❖Proton precession magnetometer (MP-2) for magnetic data collection

❖Global positioning system (GPS) to record the exact data location point and digital camera for photographing

❖Arc GIS 10.3 for the preparation of location and base map and other GIS analysis

❖Global mapper 12 and surfer 10 to post extrapolate and analyze gravity and magnetic data

❖Geo-soft for processing, presenting and interpreting of geophysical data (i.e. gravity and magnetic data)

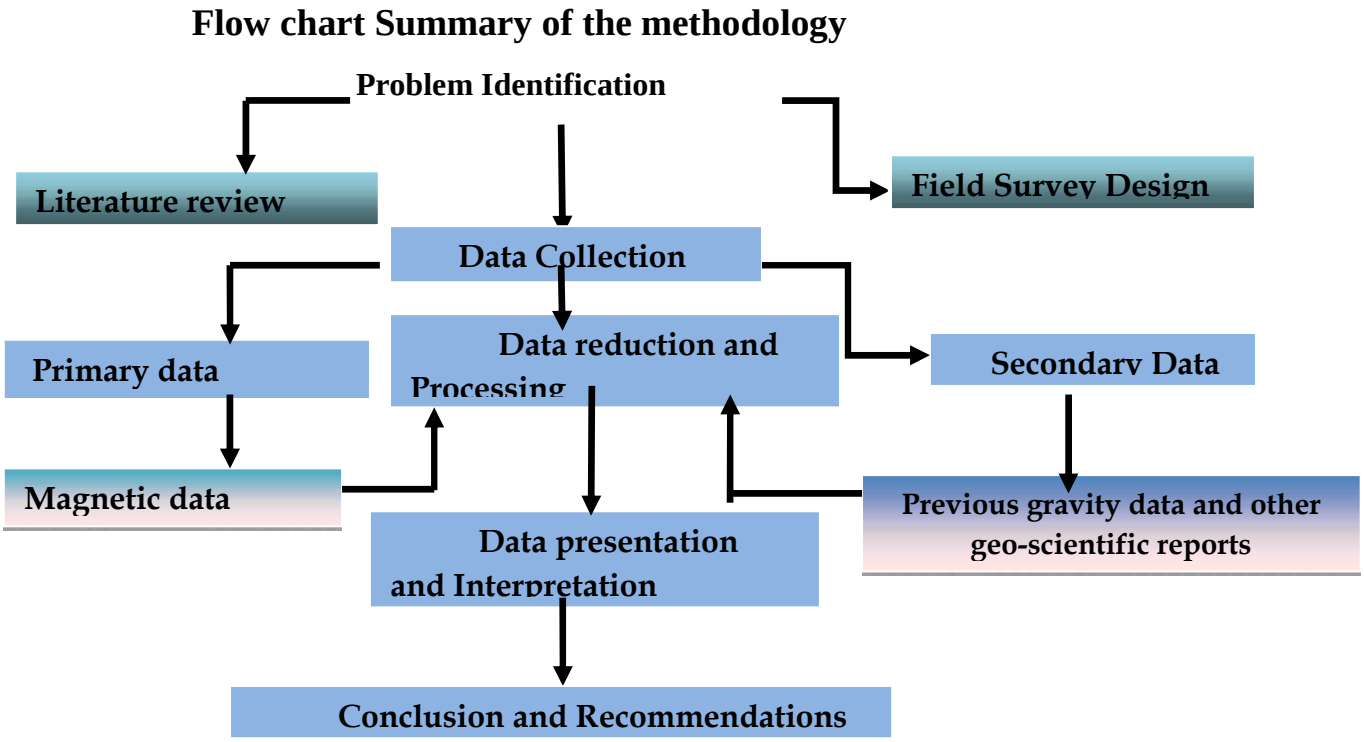

Figure 1.3 Flow Chart of the methodology used in the study

1.13 Structure of the Thesis

This MSc thesis work is organized in to Six (6) chapters. The first chapter deals with the introduction part (Including sub chapters: the Background, location of the study area, statement of the problem, objective and significance of the study, methodology employed, previous geophysical works, scope and limitations of the study and structure of the study).

Chapter two discusses about the geologic and tectonic settings of the study area. Here, the regional tectonic and geologic settings of the area in reference to the EARS in general and the MER in particular have been summarized. Geology of the study area has also been briefly summarized.

The third chapter deals with the theoretical back grounds of the geophysical methods used in the present thesis work which are compiled from various sources.

Chapter four discusses about data acquisition, reduction, processing and presentation. In this chapter, data acquiring, the type of geophysical instruments used, data processing and data presentation schemes have been discussed. Here, a number of anomaly maps have been produced and used for final interpretations.

Chapter five is concerned about results, discussions and interpretations. Here, where the different maps generated and research results are discussed and interpreted briefly.

In chapter Six, Conclusions and Recommendations regarding the results of the work are outlined.

Lastly, list of references in an alphabetical order and in the Addis Ababa University /SINET thesis format are presented.

CHAPTER TWO
2.0 GEOLOGIC AND TECTONIC SETTING OF THE STUDY AREA
2.1 Regional geological setting

The Ethiopian rift system being Active rift type, up-doming was followed by volcanism and rifting. The earliest episodes took place in the Southern Ethiopia Rift (SER) and the Afar Rifts, before 25 Ma. Rift propagation proceeded both from the south and north directions towards the MER (e.g. Bonnini et al., 2005). During the early stages of the MER, several central volcanoes erupted forming very thick pyroclastic deposits, thought to have been partially produced from fissures. These volcanic products have about 5 Ma and are known as the Nazret group (Kazmin and Berhe, 1978; WoldeGabriel et al., 1999; Boccaletti et al., 1999; Chernet et al., 1998; Abebe et al., 2005). Formation of the important rift margins of the Central MER took place about 3.5 Ma ago (e.g. WoldeGabriel et al., 1999), when the Munesa and Guraghe escarpments were formed. These escarpments are curved towards the rift and some authors considered them as the sources of the felsic pyroclastic deposits and large caldera collapses (e.g. WoldeGabriel et al., 1999). The important clue for such conclusion is that the curved escarpments of Munesa and Guraghe are related to the more than 700 m thick pyroclastic deposits that are found in both escarpments. Lithologies with age younger than 1.6 Ma are related to the NE-SW trending fracture systems together with their transversal structures that are NW-SE and ENE-WSW oriented. After 1.6 Ma the Somalian plate drifting direction changed from SE towards nearly E (Boccaletti et al., 1999, Bonnini et al., 2005, Corti, 2008, 2009), causing the development of N-S/NNE-SSW trending fracture systems known as the Wonji Fault Belt (WFB). The AVC, being a Late Pleistocene to Holocene structure, is governed by the WFB, although the transversal structures (NW-SE and ENE-WSW) also played important roles.

2.2 LOCAL GEOLOGY

The lithologic units that make up the geology of the study area consists of late tertiary silicic volcanic (Nazreth Group) overlain by a unit of fissural flood basalt – Bofa Basalt. Chilalo shield volcanoes are also belongs to the late tertiary volcanics which are represented by per alkaline basalt and trachyte. The last major event of rift faulting which has occurred in the quaternary age resulted in the formation of so many volcanic complexes called the Wonji Group. The three major volcanic complexes of the Wonji group are the Dino formation, (stratoid silicics of the rift floor), central volcanic complexes, and the fissural basalts of the rift floor. The youngest stratigraphic succession of

the study area is the Pleistocene-Holocene age lacustrine sediments which constitutes most part of the rift floor.

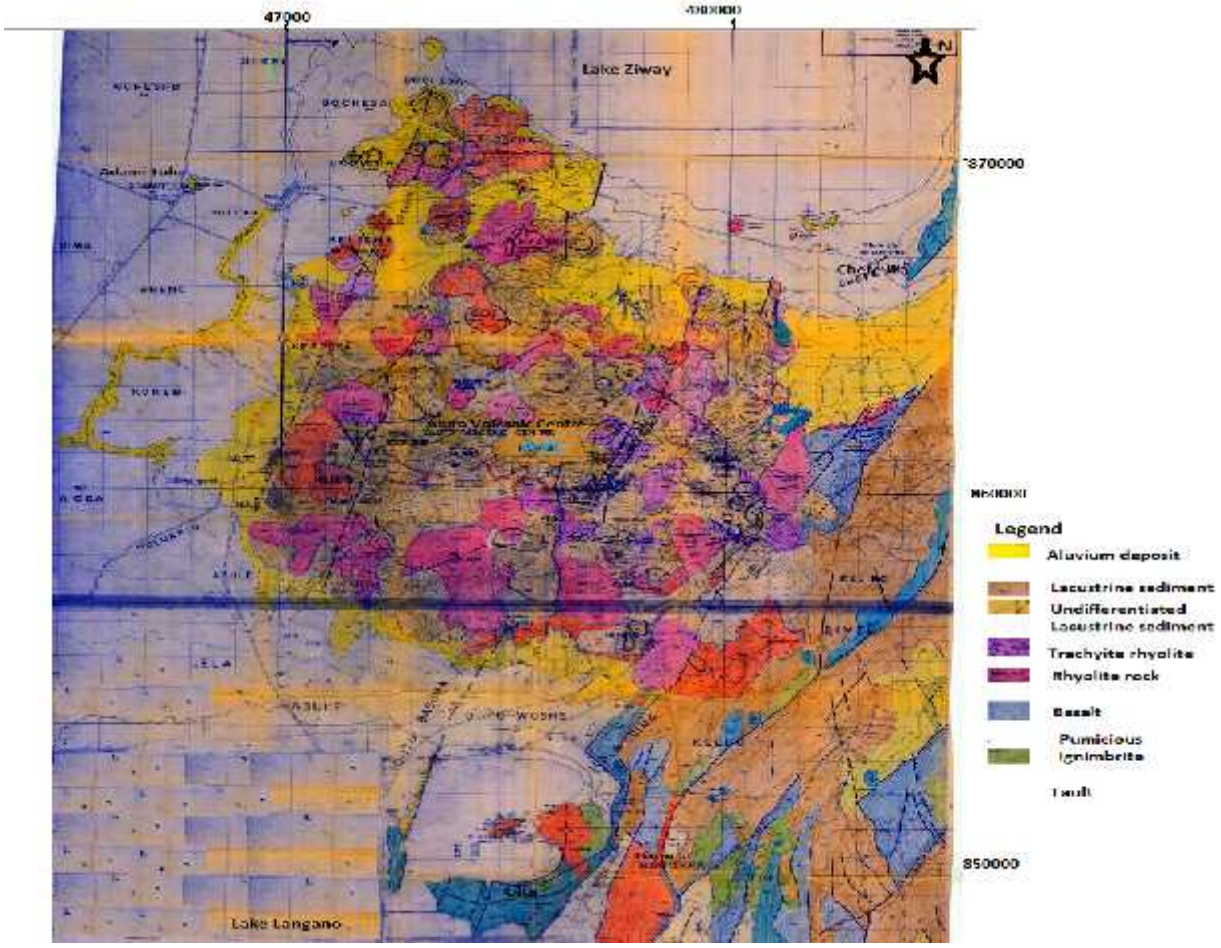

Figure 2.1 Geological map of the study area (modified from the Geological survey of Ethiopia 2012)

2.2.1 Rhyolite with some trachyte lava flows, pumice and unwelded tuffs (Qwa, Qwpu)

Most of the central volcanoes of the Wonji group are disposed along the axial zone of the rift. They are either huge conical mountains or calderas formed in the place of older volcanoes. The main volcanic centers from north to south within the rift include Aluto. Some occur on the rift floor outside the tensional belts, such as Gademotta caldera, or even on the rift shoulders, such as volcanoes and calderas. The main rock types are rhyolitic and trachytic lava flows (Qwa). In some centers alkaline and per-alkaline products are mainly represented by pumice and unwelded tuffs (Qwpu).

2.2.2 Pleistocene basalts mostly vesicular (Qwbp)

The bulk of these late basalts are concentrated in the Wonji fault belt, but there are also eruptions in the western marginal part of the rift. The basalts are clearly controlled by extensional fractures and generally display fresh aa surfaces. Chains of scoraceous cones follow the lines of fractures. These basalts are exposed at East of lake Ziway. Recent flows in many cases follow depressions of relief or flow over fault escarpment. The eruption of basalts usually followed the formation of silicic pantelleritic volcanoes, but some basalt might be contemporaneous with the earliest stages of their development.

2.2.3 Ignimbrites, tuffs, under lain pyroclastics, lacustrine beds (Qdi)

The Bofa Basalt and Nazereth Series are in most places overlain by green and gray ignimbrites with well developed fiamme and associated unwelded pyroclastic and underlain pyroclastic with occasional intercalated lacustrine beds and aphyric basalts. The pyroclastics of the Dino Formation may have sources from axial felsic volcanic eruptions complexes. The felsic lava of the Dino formation is per alkaline in composition and the ignimbrite members are not confined only to the rift floor but extensively developed on the escarpments.

2.2.4 Bofa Basalts: mildly alkaline basalts (Nbb)

The fissural basalts of this unit are aphyric locally vesicular and generally form several well defined flows with scoraceous surfaces, in places separated by paleosols. The rocks are generally weakly Structures and kinematics of the eastern margin of central Main Ethiopian rift porphyrtic, with holocrystalline ophitic ground mass with olivine, andesitic labradorite and augite. According to Tsegaye et al. (2005) the dominant lava flows in the area north of the basin are represented by plagioclase-phyric basalts with minor fine grained and scoracious varieties. Few olivine and pyroxene-phyric lava flows are reported. The basalts are generally quartz tholeites with few olivine basalts.

2.2.5 Stratoid silicics: ignimbrites unwelded tuff, ash flows, rhyolites (N1-2n)

In the study area lithologies of stratoid silicics, ignimbrites, unwelded tuffs, ash flows, rhyolites and trachytes (N1-2n) constitute a considerable portion of the rift escarpments especially in the western part near Munesa town, while in the floor they are unconformably overlapped by younger volcanic of the Dino formation. The time of formation of the Nazareth group is between 9.5 and 3 Ma years (Kazmin and Seife M., 1978). Wolde Gabriel et al., (1990) reported a thickness of more than 600 m for the Pliocene pyroclastic units in the eastern margin of the rift in the Munesa area.

2.2.6 Lacustrine Sediments, silts, clays, diatomites (Ql)

In the rift Quaternary sediments and mostly lacustrine origin are intercalated with Pliocene to Pleistocene ignimbrites both in the rift floor and rift shoulders. The older sediments are lacustrine diatomites, tuffaceous clays and silts inter-bedded with basal ignimbrites of the Nazreth Group. Structures and kinematics of the eastern margin of central Main Ethiopian rift .The lacustrine sediments are intercalated with re deposited volcanic ash and tuffs. The lacustrine sediments are mainly represented by sand and silt. The major components of the sediments are volcanic origin, such as pumice and volcanic ash, obsidian, rhyolite and basaltic rock fragments (Tsegaye et al., 2005; Bevenuti et al., 2002).

2.3 STRUCTURAL DESCRIPTION OF THE STUDY AREA

The Main Ethiopian Rift (MER) is a roughly NE-trending sector of the East African Rift system that includes a series of rift segments extending from the Afar Depression at the Red Sea-Gulf of Aden intersection to the Kenya Rift. The MER has been traditionally differentiated into three main segments: (1) the Northern (NMER), (2) the Central (CMER), and (3) the Southern (SMER), representing different stages of the extension process, from early rifting in the Southern MER to more evolutes stages in the Central and Northern MER preceding the incipient seafloor spreading in Afar. The Northern MER is considered to extend from the Afar Depression up to the Lake Koka region following the Middle course of the Awash River Valley. The Central MER encompasses most of the Lakes Region, up to the Lake Awasa area. The Southern MER extends south of Lake Awasa into the ~ 300 km-wide systems of basins and ranges, which referred to as broadly rifted zone. Faults in the Southern MER show a dominant N-S to N20° trend and were well established after ~18 Ma. The Southern MER characterizes the overlapping area between the MER and the Kenya Rift. The N-

S striking Omo and Chew Bahir basins, which are presumed to be the northward continuations of the Oligocene rift system of north Kenya are located within the Southern MER. Geophysical (gravity and seismic) investigations suggest more than 3.5 km of sedimentary fill within the basins.

2.4 TECTONIC SETTINGS

2.4.1. The NW-SE or Red Sea Trend

In the study area the NW fracture system is visible cross-cutting the NE major faults system, forming small rhombic terrains in the south-eastern parts of the AVC, in particular between Munesa and Aluto and to a minor extent in its south-central and northern parts. The south-central NW faults cross Aluto diagonally and connect several important hydrothermal manifestations, such as: Kore – Finkilo (near Jawe Artu), Oitu Artu – Adonsha.

2.4.2. The ENE-WSW or Gulf of Aden Trend

Some volcanic centers on the rift margin and within the rift itself follow the ENE trend, but are not as important as the NW-SE trend. The Aluto caldera follows the same trend. Moreover, the southern rim of the caldera is made up of a chain of volcanic centers' and craters that are elongated and aligned in an E-W direction. It is clear that the southern part of the AVC is much higher than its northern part, probably due to the fact that a northward breaching took place at Aluto before the caldera collapse.

2.4.3. The NE-SW or Ethiopian Rift Trend

In the study area the NE-SW trending faults and tectonic features are mainly expressed in the eastern and SE sectors and most of them deviate towards N, forming the NNE. Some of the volcanic centers, including the youngest three centers situated in the north-western part of the caldera, follow a NE-SW trend. This system has contributed significantly to the external and internal structural configuration of AVC. One of the important considerations refers to the fact that the older rock units, such as the Munesa crystal ignimbrite and the overlying Bofa basalt outcropping in the eastern side, are gradually lowered down to the west and in the central part of the AVC these units are found at a depth of several hundred meters.

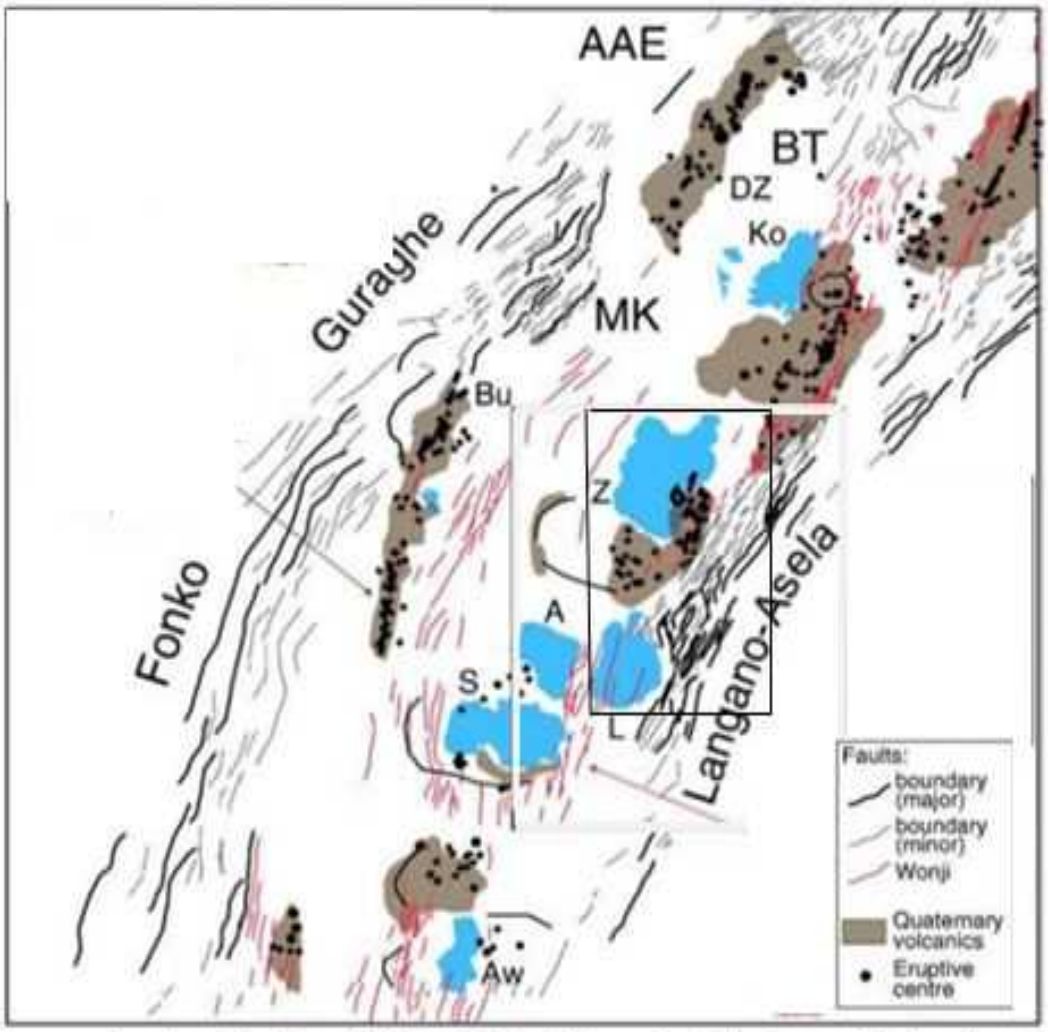

Fig **2.2** Structural setting of the Central MER . A: Lake Abiyata; Aw: Lake Awasa; Bu: Butajira volcanic chain; L: Lake Langano; S: Lake Shala; Z: Ziway.(Corti, 2009).

CHAPTER THREE

3.0 THEORY OF THE GEOPHYSICAL METHODS

3.1 GRAVITY METHOD

3.1.1 Gravity units

The first measurement of the acceleration due to gravity was made by Galileo in a famous experiment in which he dropped objects from the top of the leaning tower of Pisa (Italy). The c.g.s unit of gravity is called "Gal" which was given in honor of Galileo.

Where:

$1Gal = 1cm/s^2 = 0.01m/s^2$;

$1mgal = 10^{-3}gal = 10^{-3}\ cm/s^2 = 10^{-5}\ m/s^2$

Gravity anomalies are very small compared with the mean surface gravity value of $9.81ms^{-2}$ and are therefore often quoted in a more convenient unit, the milligal, which is equivalent to $10^{-5}\ ms^{-2}$ (10^{-3} gal).

3.1.2 Gravity corrections

For most geophysical methods, it is necessary to apply a variety of corrections to the raw data obtained in the field in order to reduce or prepare the data for further enhancement and interpretation (Dentith and Mudge, 2014)

In gravity work, more than in any other branch of geophysics, large and in principle calculable effects are produced by sources that are not of direct geological interest (Milsom and Eriksen, 2011). For example, the value of the observed gravity "g_{ob}"at a given observation point is affected by a number of factors such as the elevation above mean sea level where the point is located, the latitude in which the point is located, the topography of the area in which the measurement is taking place, etc. These effects are removed by reductions that involve the sequential calculation of a number of recognized quantities. In each case, a positive effect is one that increases the magnitude of the measured field and the sign of the reduction is opposite to that of the effect it is designed to remove (Milsom and Erikson, 2011). This process is known as gravity reduction (Kearey et al., 2002 as cited in LaFehr, 1991) or reduction to the geoid as the sea level is usually the most common datum level, although the datum plane need not necessarily be the mean sea level (Dobrin, 1988).

Although most corrections are spatial, some are to allow for factors that change the reading when the gravimeter is at the same location (Mussett and Khan, 2000). Drift and Earth Tide correction types are time dependent; whereas the spatial type of corrections are related to variations in distance from the center of the earth. Accordingly, first the time dependent corrections and then the space dependent corrections will be explained next.

3.1.2.1 Instrumental drift correction

The basis for instrumental drift correction arises from the fact that gravimeter reading change (drift) with time as a result of elastic creep in the springs, producing an apparent change in gravity at a given station (Reynolds, 1997). Correction for instrumental drift is thus, based on repeated readings at a base station at recorded times throughout the day (Kearey et al., 2002). The base station is commonly revisited at every 1-2 hours (Reynolds, 1997).

The differences between successive measurements at the same station are plotted to produce a drift curve and the observed gravity values from intervening stations can be corrected by subtracting the amount of drift from the observed value (Reynolds, 1997). Drift is assumed to be linear between consecutive base readings. (Kearey et al., 2002)

3.1.2.2 Tidal drift correction

Tidal Effect is the variations in gravity observations resulting from the attraction of the moon and sun and the distortion of the earth so produced. Superimposed on instrument drift is another temporally varying component of gravity.

3.1.2.3 Latitude correction

The need for latitude correction arises from two effects (Telford et al., 1990): First, since the earth rotates around its axis and this rotation tends to produce a centrifugal acceleration force which opposes the effect of the gravitational acceleration. This centrifugal acceleration is maximum at the equator and zero at the poles. Second, due to the imperfect spherical shape of the earth (i.e. flattened at the poles and bulged at the equator), a variation in both equatorial and polar radii arise. This phenomenon gives rise to gravity value variation with distance from the center of the earth.

The latitude correction is thus applied in order to account for these two effects. The average value of gravity for a given latitude (θ) is approximated by the 1967 reference gravity formula, adopted by the International Association of Geodesy (Lillie, 1999).

$$\mathbf{g_t = g_e(1 + 0.005278895 \sin^2 \theta + 0.000023462 \sin^4 \theta)} \quad \textbf{(3.6)}$$

Where:

$\mathbf{g_t}$ = Theoretical gravity for the latitude of the observation point (mGal)

$\mathbf{g_e}$ = Theoretical gravity at the equator (978031.85 mGal)

θ = Latitude of the Observation Point (Degrees)

3.1.2.4 Free air correction

The need for free air correction (FAC) emanates from the fact that gravity varies inversely with the square of distance from the center of the earth. Hence, it is necessary to correct for changes in elevation between stations to reduce field readings to a datum surface (Telford et al., 1990).

It is the allowance for the reduction of the magnitude of gravity with height from the center of the earth irrespective of the nature of the rock between the observation point and the center of the earth (Reynolds, 1997; Telford et al., 1990).

The change in gravity (Δg) with increasing distance from the center of the earth (ΔR) is given by the first derivative of "g" with respect to "R" (Lillie, 1999):

$$\lim_{\triangle Rappr0} = \frac{\triangle g}{\triangle R} = \frac{dg}{dR} = -\frac{2}{R}\frac{GM}{R^2} = \frac{-2}{R}(g)$$

$$\frac{dg}{dR} = \frac{-2g}{R}$$

Assuming average value of: $g = 980.625 \text{mGal} \;\&\; R = 6.367 \text{km} = 6367.000 \text{m}$

$$\mathbf{\frac{dg}{dR} = \frac{-2g}{R} = -0.308\, mGal/m} \quad \textbf{(3.7)}$$

Where:

$\frac{dg}{dR}$ = Average value for the change in gravity with increasing elevation

The above equation (3.7) illustrates that for approximately every 3m upward from the surface of the Earth, the acceleration due to gravity decreases by about 1mGal (Lillie,1999).

3.1.2.5 Bouguer correction

Even after elevation correction is made, gravity reading varies from station to station due to differences in mass between the observation point and the sea level datum (Lillie, 1999). The Bouguer correction (BC) is thus, to account for the attraction of material between the station and the datum plane that was ignored in the free air correction (Telford e al.,, 1990).

Bouguer correction is done by approximating the mass as an infinite slab, with thickness (h) equal to the elevation of the station (Lillie, 1999). The attraction of such slab is:

$$\mathbf{BC\ Z\ 2°rGh} \qquad \mathbf{(3.8)}$$

Where:

BC= Bouguer Correction

ρ= Density of the Slab

G= Universal gravitational Constant

h = Thickness of the slab

Substituting the values of G and 2ρ in equation (3.8) yields:

$$\mathbf{BC = 0.0419\rho h} \qquad \mathbf{(3.9)}$$

Taking the average crustal density of 2.67 g/cm^3 and substituting it in the above equation (3.9) yields:

$$\mathbf{BC = 0.112(mGal/m)h} \qquad \mathbf{(3.10)}$$

It can be seen from equation (3.10) that, for every 9 meter of surface elevation, the increased mass below the observation point adds about 1mGal to the observed gravity. (Lillie, 1999). The Bouguer correction is subtracted from the observed gravity value if the station is above the datum plane and is added when the station is below the sea level.

3.1.2.6 Terrain correction

The Bouguer correction assumes that the rock occupying the height interval between the datum level and the station is a uniform slab extending to infinity in all directions (Dentith and Mudge, 2014). In other words, the land surface is assumed to be represented by a subdued topography (i.e. the terrain around the observation point is perfectly flat). In reality, there exist “hills” (mountains) rising above the observation point and “valleys” below the observation point.

According to Telford et al., (1990), the terrain correction is thus, to allow for surface irregularities in the vicinity of the observation point. Hills above the elevation of the gravitation station exert an upward pull on the gravimeter, where as valleys (lack of material) below it fail to pull down ward on it. Thus, both types of topographic undulations affect gravity measurements in the same sense as a result of which, the terrain correction is usually added to the observed gravity reading (e.g. Dobrin, 1988; Telford et al., 1990; Reynolds, 1997).

3.1.3 Gravity Anomaly

Gravity observations can be used to interpret changes in mass below different regions of the Earth. To see the mass differences, the broad changes in gravity from equator to pole must be subtracted from station observations by predicting the gravity value for a station's latitude (theoretical gravity), then subtracting that value from the actual value at the station (Observed gravity), yielding a gravity anomaly (Lillie, 1999).

A discrepancy between the corrected, measured gravity and the theoretical gravity is called a gravity anomaly (Lowrie, 2007). It arises because the density of the Earth's interior is not homogeneous. The most common types of gravity anomalies are the Bouguer anomaly and the free-air anomaly.

3.1.3.1 Free air gravity anomaly

The free air gravity anomaly (ΔgF_A) takes in to account the latitudinal change in gravity on the Earth's best fitting ellipsoid represented by the theoretical gravity (g_t) and the vertical change in gravity between the reference datum and the observation height assuming that the gravity station is located in free air, hence the name free air anomaly (Hinze et al., 2013).

Lillie (1999) defined free air gravity anomaly as the observed gravity (g_{obs}) corrected for latitude and elevation of the station. The free air gravity anomaly is mathematically calculated as:

$$\Delta gF_A = g_{obs} + FAC - g_t \qquad (3.11)$$

Where:

ΔgF_A = Free air gravity anomaly

g_{obs} = Observed gravity

FAC = Free air Correction

g_t = Theoretical Gravity

From equation (3.11), two things can be understood (Lillie, 1999):

1. Subtracting the theoretical gravity from the observed gravity corrects for the latitude, thus accounting for the spin and bulge of the earth
2. Adding the "FAC" puts back the gravity lost to elevation, there by correcting the increased radius "R" from the Earth's center.

3.1.3.2 Bouguer gravity anomaly

The Bouguer gravity anomaly, like the free air gravity anomaly reflects changes in mass distribution below the surface, except the Bouguer anomaly has had an additional correction, removing the effect of mass above sea level datum on land (Lillie, 1999).

The Bouguer gravity anomaly is the most frequently used of the gravity anomalies in surveys of continental and in near shore marine areas (Hinze et al., 2013).

The variation of the Bouguer anomaly should reflect the lateral variation in density such that a high density feature in a lower density medium should give rise to a positive (+Ve) Bouguer anomaly. Conversely, a low density feature in a high density medium should result in a negative (-Ve) Bouguer anomaly (Reynolds, 1997).

The simple Bouguer gravity anomaly (ag_{Bs}) on land is computed from the free air gravity anomaly (Lillie, 1999).

$$ag_{Bs} = agFA - (0.112\,mGal/m)h \qquad (3.12)$$

Where:

h= the elevation in meters.

3.2 MAGNETIC METHOD

3.2.1 General

Like the gravity method, the magnetic method is a passive geophysical exploration technique in that it is based on mapping the natural or normal magnetic force field of the Earth (Hinze et al., 2013).

The aim of a magnetic survey is to investigate subsurface geology on the basis of anomalies in the earth's magnetic field resulting from the magnetic properties of underlying rocks (Kearey et al., 2002).

The method has undergone various historical developments. Telford et al., (1990) for example, have compiled the historical perspectives of the method which is not summarized here. But, above all, the introduction of digital recording and processing of magnetic data and interpretation algorithms have improved the tedious procedures that involve reducing magnetic data in to maps.

Throughout the course of its development, the method has been used for a variety of applications ranging from Archaeological and Engineering site investigations, to exploration for economic resources and studies of crustal tectonic structures and processes (Hinze et al., 2013).

3.2.2 Nature of earth's magnetic field

Although there are several parts of the geomagnetic field of the earth, the following three are important as far as exploration geophysics is concerned (Telford et al., 1990).

A. Main field
   - This field varies relatively slowly and is of internal origin.

B. A small field
   - Compared to the main field, it varies rapidly and originates outside of the earth.

C. Spatial variations of the main field
   - Usually smaller than the main field which is nearly constant in time and space. They are caused by local magnetic anomalies in the near surface crust of the earth and are targets of magnetic surveying.

3.2.3 Temporal variations of earth's magnetic field

A. Secular variations

- These are longer period variations of the Earth's magnetic field of usually greater than a year (Mudge and Dentith, 2014). Although their mechanism is not understood well, several theories indicate that they are due to changes in electric currents producing the internal field (e.g. Dobrin and Savit, 1988; Mudge and Dentith, 2014)
- There are also variations in the inclination and declinations of the field; in which the geomagnetic field of the earth has reversed its polarity a number of times in the geologic

time as revealed from a number of paleomagnetic studies, with the most recent one occurred about 700000 years ago (Mudge and Dentith, 2014).

A. Diurnal variations

- These are smaller but more rapid oscillations in the earth's field with a period ranging about a day and amplitude averaging 25 Gamma (Dobrin and Savit, 1988).
- They are due to changes in the external field related to sources external to the earth. These are chiefly due to electric currents flowing in the ionosphere, the ionized layer of the upper atmosphere, and are associated with radiation from the Sun (Dentith and Mudges,2014)
- They are of direct significance to magnetic prospecting

B. Magnetic Storms

- These are rapid variations of the field with periods of milliseconds to minutes appearing as irregular bursts lasting from hours to several days (Dentith and Mudges,2014)
- Magnetic surveying must stop in such events, as they occur so rapid and in unpredictable way that correcting their effects is not feasible (Dobrin and Savit, 1988)
- They correlate with sun spot activity and cause a wide range of amplitude changes, up to 1000nT at most latitudes and even greater at the poles (Dobrin and Savit, 1988)
- Magnetic storms make magnetic surveying impractical because the target anomalies related to the crustal rocks are often smaller in amplitude than these erratic variations(Dentith and Mudges,2014)

3.2.4 Magnetization and magnetic susceptibility of materials

3.2.4.1 Magnetization

If a body is placed in an external magnetic field (also called inducing field), it acquires although usually small, a magnetization which is proportional to the inducing field (Milsom, 2003). The relationship is given as:

$$\mathbf{M} \propto \mathbf{H}$$

(The magnetization acquired is directly proportional to the induced field)

$$\mathbf{M} \; Z \; ¡ \mathbf{H}$$

Where

M = Magnetization acquired by the material

χ = Magnetic susceptibility of the material

H = Inducing field

3.2.5 Measuring magnetic field strength and measuring Instruments

According to Dentith and Mudge (2014), magnetic objects alter the strength and direction of the Earth's magnetic field. Changes in the field's direction due to most geological features are very small and offer very little resolution in detecting variations in the magnetic properties of the subsurface. However, the effect on field strength is significant and is by far the most sensitive element to changes in the magnetic properties of crustal rocks. It is the strength of the magnetic field that is measured and mapped in magnetic surveying.

Although a number of devices have been developed and used since the first century AD, magnetometers used specifically in exploration geophysics can be classified in to three categories (Reynolds, 1997). These are: The torsion (and balance); Fluxgate and Resonance types, of which the first has been superseded by the latter two.

The resonance type magnetometers are also classified in to: The proton Precession magnetometer and Alkali- vapor magnetometer, both of which monitor the precession of atomic particles in an ambient magnetic field to provide an absolute measure of the total magnetic field (Reynolds, 1997).

The proton precession magnetometer (usually abbreviated as proton magnetometer) measures the total strength of the magnetic field, but not its direction and so shows a total field anomaly, also called a total intensity anomaly (Mussette and Khan, 2000).

The fluxgate magnetometer on the other hand, measures the strength of magnetic field in a particular direction. As a result of which, the fluxgate magnetometer is in essence a vector magnetometer and finds applications where the direction to a magnetic source is required, such as down hole magnetometer and down hole electromagnetic (Dentith and Mudge, 2014).

3.2.6. Magnetic data reduction

The reduction of magnetic survey data is principally aimed at removing the effects of temporal variations in the Earth's magnetic field that occur during the course of the survey. Like gravity reduction, planetary-scale spatial variations in the field are compensated for, but in contrast, elevation-related variations in the magnetic field are minor.

As the Earth's magnetic field varies from nearly 25,000nT at the magnetic equator to 69000 nT at the poles, the increase with magnitude needs to be taken in to account (Reynolds, 1997). Survey data at any given location can be corrected by subtracting the theoretical field value (F_{th}), obtained from the International Geomagnetic Reference Field (IGRF) from the measured observed value (F_{obs})

To remove all causes of magnetic variation from the observations other than those arising from subsurface geology it is necessary to make a correction to the magnetic raw data.

3.2.7 Magnetic data Correction

3.2.7.1 Diurnal variation correction

The effects of diurnal variation may be removed in several ways. On land the magnetometer is read at a fixed base station periodically throughout the day. The differences observed in base readings are then distributed among the readings at stations occupied during the day according to the time of observation. Magnetometers do not drift and base readings are taken solely to correct for temporal variation in the measured field (Kearey et al., 2002).

3.2.7.2 Geomagnetic correction

In order to produce a magnetic anomaly map of a region, the data have to be corrected to take in to account the effect of latitude and to a lesser extent longitude (Reynolds, 1997).Survey data at any given location can be corrected by subtracting the theoretical field value B_{th}, obtained from the International Geomagnetic Reference Field (IGRF) from the measured value, B_{ob}. Therefore, the magnetic anomaly (ΔB), obtained by subtracting the diurnal correction ($¢_D$) and geomagnetic correction (B_{th}) is given by

$$\Delta B = B_T - ¢ B_D - B_{th} \quad (3.14)$$

CHAPTER FOUR

4.0 DATA ACQUISITION AND REDUCTION

4.1 General

This work has utilized gravity and magnetic methods. The data for gravity are secondary in that they were acquired from previously collected. On the other hand, the magnetic data are both secondary and primary data. The primary magnetic data were collected by the researcher and his advisor during the field season (January, 2017).

All the gravity and magnetic data utilized in this work were collected in a random distribution fashion. The selection of the survey patterns in effect has taken the accessibility of study area, scale of the study, time and financial constraints and others in to account.

In all of the above methods, the field measurements have been recorded using a field recording format in at least three attributes (geographic coordinates in terms of Easting and Northing, Elevation or height above mean sea level) and the anomaly reading associated with each geophysical method employed. Accounts of the data acquisition and consequent reduction processes associated with each geophysical method are summarized as follows.

4.2 THE GRAVITY DATA

4.2.1 Gravity data reduction

The gravity data reduction processes in the present work was aimed at transforming the raw data sequentially in to a data table of final complete Bouguer anomaly values by correcting the variations in the earth's gravitational field which don't result from the differences of density in the underlying rocks.

Accordingly, all the stations occupied in the present work have been referred to the International Gravity Standardization Net71 (IGSN 71) gravity datum. The theoretical gravity has been computed using the 1967 gravity formula (Geodetic reference system 1967). All the necessary standard correction types have been made, based on the standard gravity data correction procedures outlined in section 3.1.3 of chapter three.

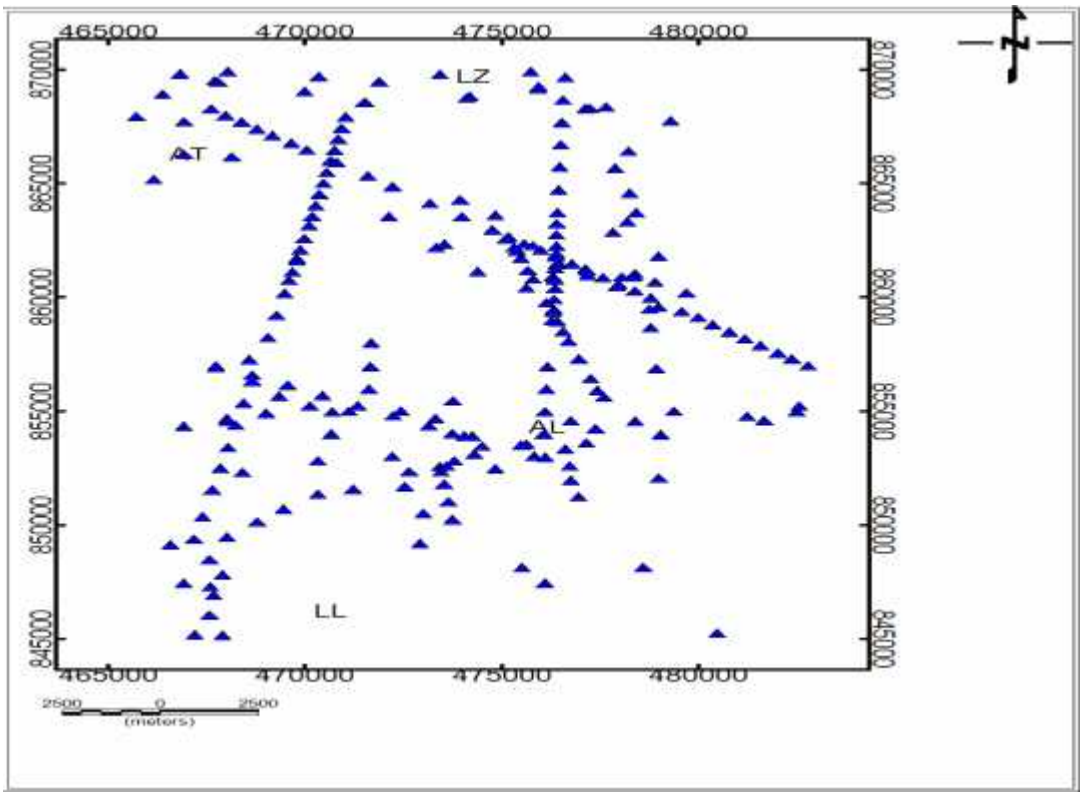

Figure 4.1 Gravity data distribution map of the study area

4.3 THE MAGNETIC DATA

4.3.1 Magnetic data acquisition

The magnetic data utilized in the present thesis work which amount to a total of 130 (as indicated in the magnetic data location plot map, Fig. 4.2); were collected using a Proton Precession Magnetometer of MP2 type that measures the total intensity of earth's magnetic field at a given observation point, with an accuracy of one Gamma (1^{γ}).

The survey was conducted in a random type, with the geographic coordinates and elevation of each observation point determined using a hand held GPS of Garmin 12 type.

Before any measurement was made, a base station for all the observations occupied was established for the purpose of correcting the diurnal effect. Accordingly, all the primary magnetic data were collected from the survey and were made available for further reduction and processing steps.

4.3.1 Magnetic data reduction.

The raw magnetic data collected in the field and those obtained secondary data are transformed to total magnetic field anomaly values by applying diurnal correction and IGRF correction using the standard ground magnetic data reduction procedures in order to compute the total magnetic anomaly values of all the stations considered in the study area.

The computed total magnetic field anomaly values of the stations considered in the study area were plotted to compile the total magnetic field anomaly map (Fig 5.6) of the study area, which is the sum of the effects of both the regional and residual fields was then used for further processing; as for example in separating the regional and residual field effects. Consequent processing and enhancements were based largely on the residual magnetic field anomaly map generated using high pass filtering techniques applied in Oasis Montaj Soft ware (V.6.4.2).

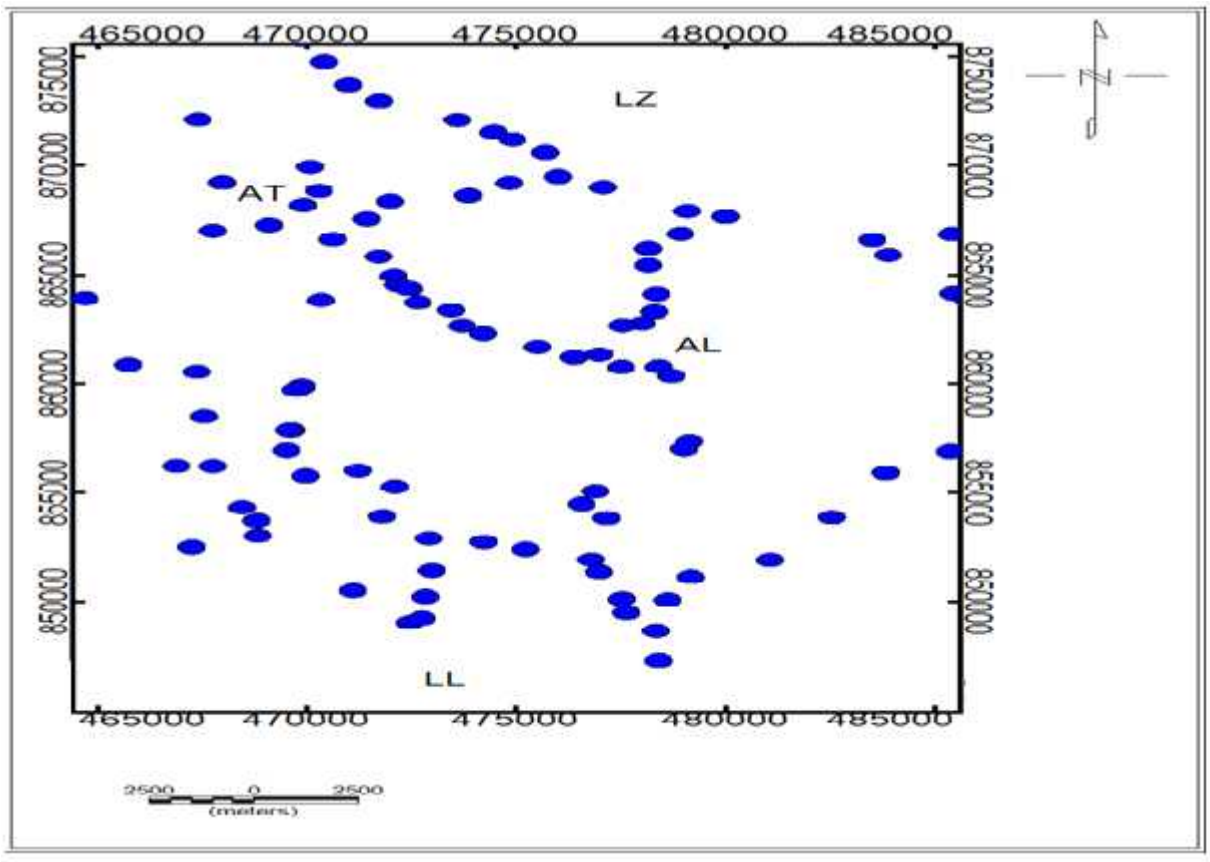

Figure 4.2 Magnetic data distribution map of the study area

4.4 DATA PROCESSING AND PRESENTATIONS

4.4.1 Gravity data processing and presentations

In the present thesis work, after the necessary reductions and allowances for the effects of such as latitude, elevation, slab and terrain have been made to the raw gravity data. The complete Bouguer anomaly and its derivative anomalies have been computed using the Geosoft Oasis Montaj software (V 6.4.2).

For better processing, presentation and interpretations, the Geosoft Oasis Montaj software prefers field data to be acquired in closely spaced stations and in a square grid type. To achieve this, the software in its first step performs gridding of the field data using different methods.

In the present thesis work, the computed point gravity anomaly values were gridded using the minimum curvature gridding method so as to interpolate the field data on to a regular, square grid using an average grid cell size of 2000 m. A complete Bouguer anomaly map (Fig. 5.1) was finally generated by using the complete Bouguer anomaly value column as gridding column, which was used then as the final gravity anomaly map base for further filtering processes, enhancements and interpretations regarding the lateral subsurface density variations.

The complete Bouguer anomaly map (Fig. 5.1) generated represents the sum of the regional (deep seated) and local (residual) anomalies which arise from responses of the large, deep seated and local, shallow depth geologic materials and structures, respectively. Hence, there is a need to separate the responses of both regional and local features from the complete Bouguer anomaly data for effective and better interpretations of the intended research objectives.

Accordingly, following the gridding and complete Bouguer anomaly map generation step, the residual and regional anomaly separation process of the gravity data was accomplished using the low and high pass filtering methods using Geosoft OasisMontaj Software (V 6.42).

Accordingly, the regional gravity anomaly map (Fig 5.2) was generated using the Geosoft Oasis Montaj Software by subtracting the residual gravity anomaly data from the complete Bouguer anomaly data.

After the separation of the residual and regional anomalies, different data enhancements and filtering techniques have been applied including respective maps such as Horizontal gradient map (Fig. 5.4) and Euler depth solutions for SI= 0.5 (Fig. 5.5) are generated, discussed and interpreted.

4.4.2 Magnetic data processing and presentations

The magnetic data utilized in the present work have undergone through series of data reduction steps before they were subjected to the data processing and presentations phases.

Accordingly, corrections on the daily variations (Diurnal correction) and the effect of the core field (IGRF- removal) on the measured (Observed) total magnetic intensity anomaly values have resulted in diurnally corrected total intensity anomaly and IGRF corrected total intensity anomaly values, respectively. It was the IGRF corrected anomaly values taken as a final and base anomaly values for generating the IGRF corrected anomaly map using the Geosoft Oasis Montaj Software (V 6.42) in which, further enhancements , filtering operations and interpretations have been based.

The IGRF corrected total magnetic intensity anomaly map, like the complete Bouguer anomaly map in the gravity survey, represents the sum of the effects of the shallow depth, short wave length and deep seated, long wave length source effects. Hence, effective interpretations of the magnetic data necessitate the separation of the regional and residual responses from the IGRF corrected total magnetic intensity anomaly values.

Following the separation of the regional and residual magnetic anomalies using the same procedures as applied in the gravity data, further filtering techniques and enhancements were performed as per the procedures of the magnetic data processing steps.

CHAPTER FIVE

5.0 RESULTS AND INTERPRETATIONS

5.1 The Gravity survey results and interpretations

5.1.1 Complete Bouguer anomaly map

The Bouguer gravity anomaly reflects changes in mass distribution below the surface, except the Bouguer anomaly has had an additional correction, removing the effect of mass above mean sea level datum on land (Lillie, 1999).

The variation of the Bouguer anomaly should reflect the lateral variation in density, such that a high density feature in a lower density medium should give rise to a positive Bouguer anomaly. Conversely, a low density feature in a high density medium should result in a negative Bouguer anomaly (Reynolds, 1997).

The Bouguer anomaly map (Fig. 5.1), included in this work was produced by gridding the final reduced observed gravity readings of each observation station following the reduction processes described elsewhere in this work. Again, Geosoft Oasis Montaj Soft ware (V.6.4.2) was employed in generating this map. A grid cells extended beyond data =2000 was used.

A first analysis of the complete Bouguer anomaly map (Fig. 5.1) indicates that the gravity responses reflect the heterogeneity in the subsurface density distribution beneath the survey area.

The observed gravity anomaly values range from a minimum of -198 mgal to a maximum of -177 mgal in the study area. The anomaly map further reveals three distinct anomaly zones, which include the medium to very high central anomaly zone which is oriented in a NNW to SSE direction and a medium to very low negative anomaly zones located in the Northeastern, eastern and south eastern part of the study area.

The positive peak (-177 mgal) which corresponds to the location of the Aluto volcanic centre may thought to be caused by high density volcanic products. The positive peak (-177 mgal) which corresponds to the location of the Adami Tulu locality is thought to be caused by high density rhyolite intrusions.

The relatively low anomaly (-198 mgal) observed over the study area are thought to be caused by low density sedimentary depositions occurring at the southern shore of Lake Ziway and northern shore of Lake Langano.

The medium negative gravity anomaly (≈ -185 mgal) observed over the summit of the Aluto volcanic complex being superposed on the positive one is thought to be caused by the sedimentary deposit of the caldera and the volcanic ash and pyroclastic materials on the top of the mountain.

Since the Complete Bouguer anomaly includes effects from sources of a local and shallow nature as well as regional and deep structures, these effect are described in the following section.

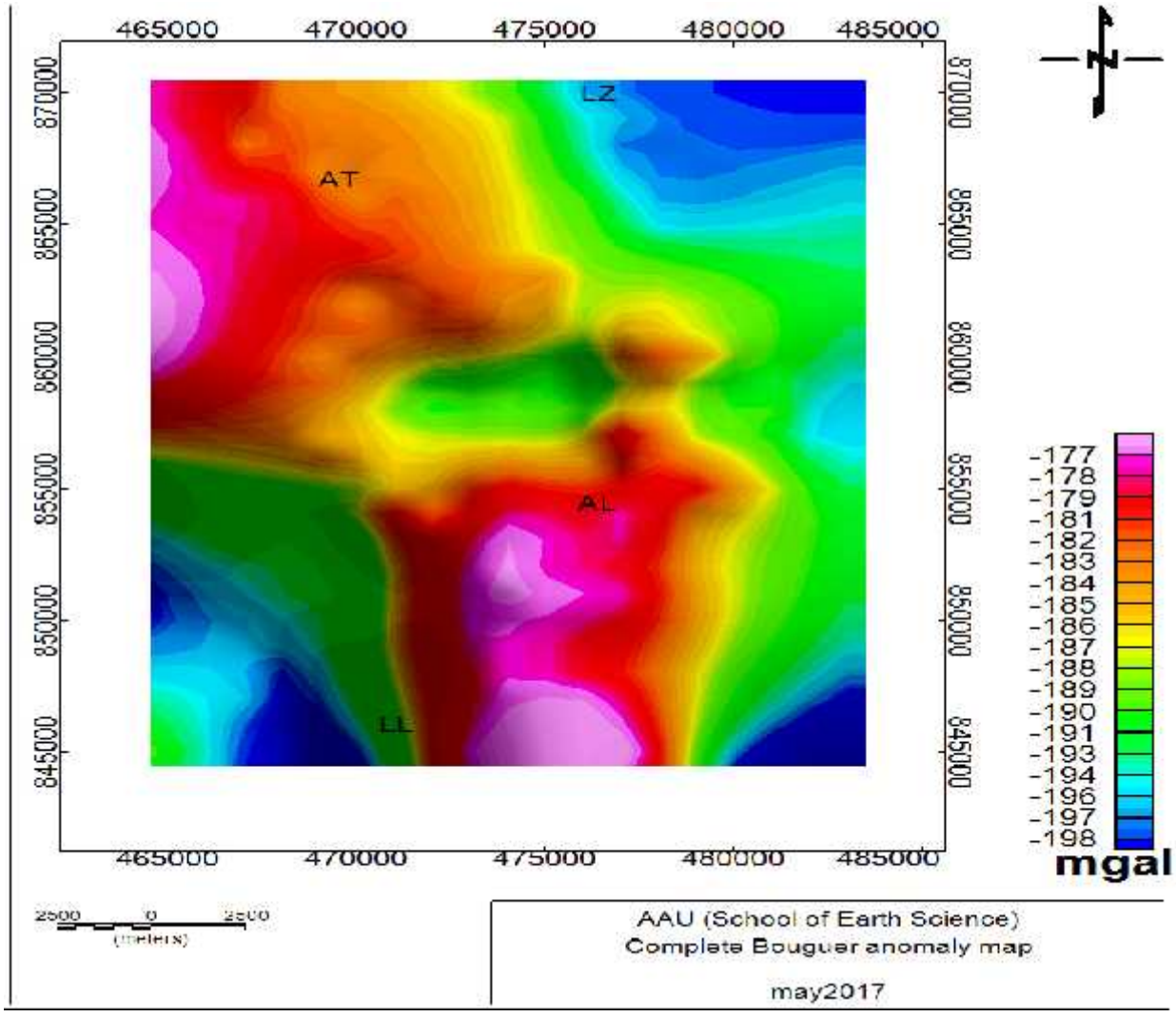

Figure 5.1 Complete Bouguer anomaly map

5.1.2 Regional gravity anomaly map

The complete Bouguer anomaly map consists the sum of the effects of features of long wave length, deep seated (regional anomaly) and the near surface, short wave length (residual anomaly) components. Separation of these components is important to determine the effects of the deep seated and the shallow depth sources contributing for the complete Bouguer anomaly value.

Despite the availability of various methods of anomaly separation, a low pass filtering with a cutoff wavelength 10 km was applied to the complete Bouguer anomaly for generating the regional Bouguer anomaly using Geosoft Oasis Montaj (V 6.4.2) based on the following series of steps.

During filtering, increasing the separation between the source and detector cause a decrease in amplitude and increase in wave length of the response, where the rate of attenuation of amplitude is wave-length dependent (i.e. Shorter wavelengths, high frequencies associated with near-surface sources attenuate more rapidly with height than the longer wavelengths and lower frequencies sources. Hence, shorter wave length, shallow- sourced responses plus any short wave length noises are suppressed and longer wave length responses dominate the filtered data (Dentith and Mudges, 2014, pp. 12).

The Regional anomaly map (Fig 5.2) reveals three prominent anomaly zones which are similar to those of the complete Bouguer anomaly map (Fig. 5.1). The only difference between them is that the anomaly features observed in regional anomaly map are smooth and elongated indicating that the effects of deep seated anomalous geologic structures. Since this MSc thesis is devoted to the investigation of subsurface shallow structures so a detailed interpretation of the regional gravity anomaly map is not considered here.

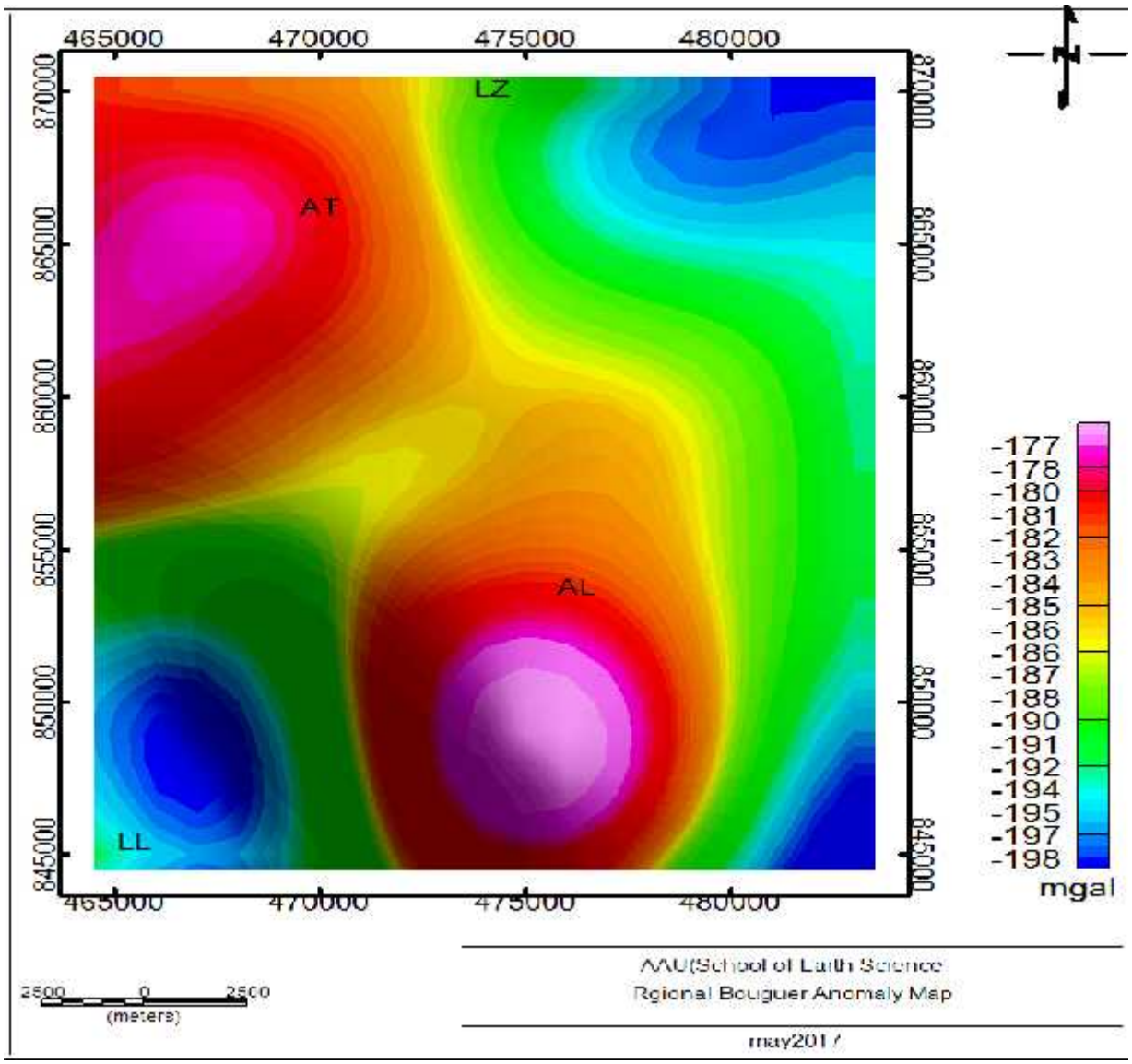

Figure 5.2 Regional gravity anomaly maps

5.1.3 Residual gravity anomaly map

The residual gravity field anomaly map was generated after the separation of the regional Bouguer gravity anomaly value from the complete Bouguer anomaly value following the use of the high pass filtering methods with a cutoff wavelength 10 Km using Geosoft Oasismontaj software (V 6.4.2).

This map is expected to reveal the gravity anomalies resulting from shallow depth anomalous geologic structures in the subsurface.

The residual Bouguer anomaly map is dominated by a number of positive and negative short wave length anomalies occurring as patches of circular and elliptical features aligned almost in NE-SW and NNW-SSE directions. The positive highs in the study area coincide with the locations of high density volcanic products of the Aluto volcanic center and the Adami Tulu locality in the area are attributed to the presence of dense intrusions associated with these young silicic volcanoes.

The circular lows which appear to be surrounded by the highs could be the expression of thick accumulation of the rift floor sediments.

The central low which is surrounded by the highs of the Aluto high density volcanic products is interpreted as the effect of the sedimentary deposit of the Aluto caldera and the volcanic ash and the pyroclastic materials on the top of the mountain.

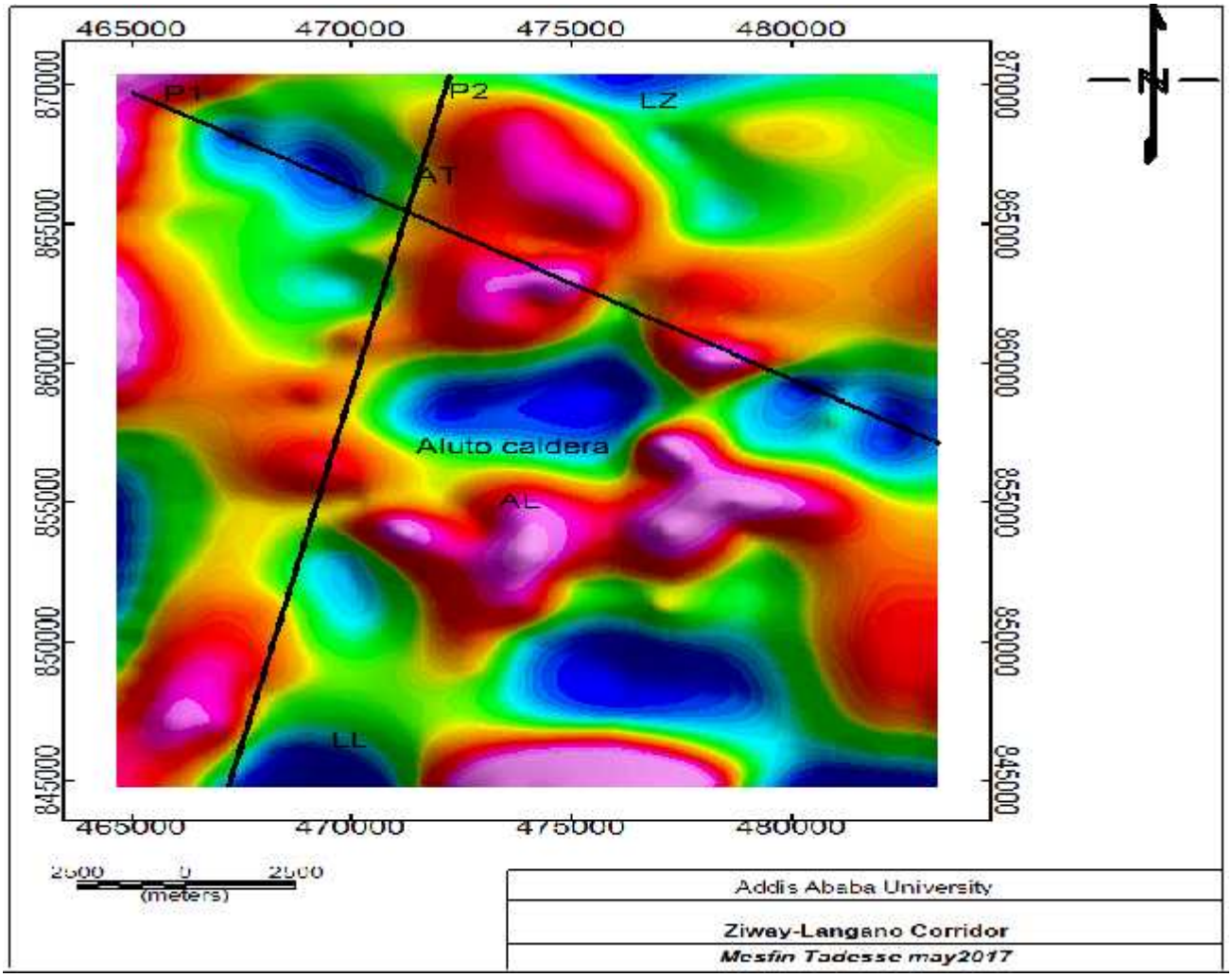

Figure 5.3 Residual gravity anomaly maps

5.1.4 Horizontal gradient gravity map

The horizontal gradient is a mathematical anomaly enhancement method that can be computed by:

$$HG = HG(x, y) = \sqrt{(\frac{\partial \Delta g}{\partial x})^2 + (\frac{\partial \Delta g}{\partial y})^2}$$

Where Δg is the resisdual anomaly,

The horizontal gradient method is used to locate the boundaries of regions of contrasting density from gravity data. The method is based on the premise that the maximum horizontal gradient of the observed gravity anomaly, which is caused by a planar anomalous body, tends to overlie the edges of the body (Fig. 5.4). Note also that the edges mark locations of the contacts indicating that the HG method is designed to inspect fault and contact features.

Horizontal gradient map can produced from gridded residual gravity anomaly map data using the Geosoft OasisMontaj software. The compiled HG map is judged to be simple, interesting and a reputable end result which reveals the anomaly texture and highlight anomaly-pattern discontinuities. The HG maxima identified on such maps can be inspected to assist in the location of linear structures such as faults and lineaments.

The horizontal gradient gravity map (Fig 5.4) of the survey is compiled from the gridded residual gravity anomaly data. The map reveals lineated maximum horizontal gradient anomalies which are dominantly oriented in the N-S direction.

Locations of the maximum horizontal gradient magnitude are shown with black lines superposed along their orientation (Fig5.4). The high horizontal magnitude plots outline lateral mass heterogeneities which are thought to be the expressions of lithological and structural boundaries.

The high gradient magnitudes plots trace linear features trending N-S, The linear features are attributed to faults and fractures, and their continuities are observed in the study area. Moreover the N-S trending linear features (faults and fractures) revealed by the horizontal gradient map can be considered to be the major geologic structures that favor the flow of ground water within lake Ziway to Lake Langano.

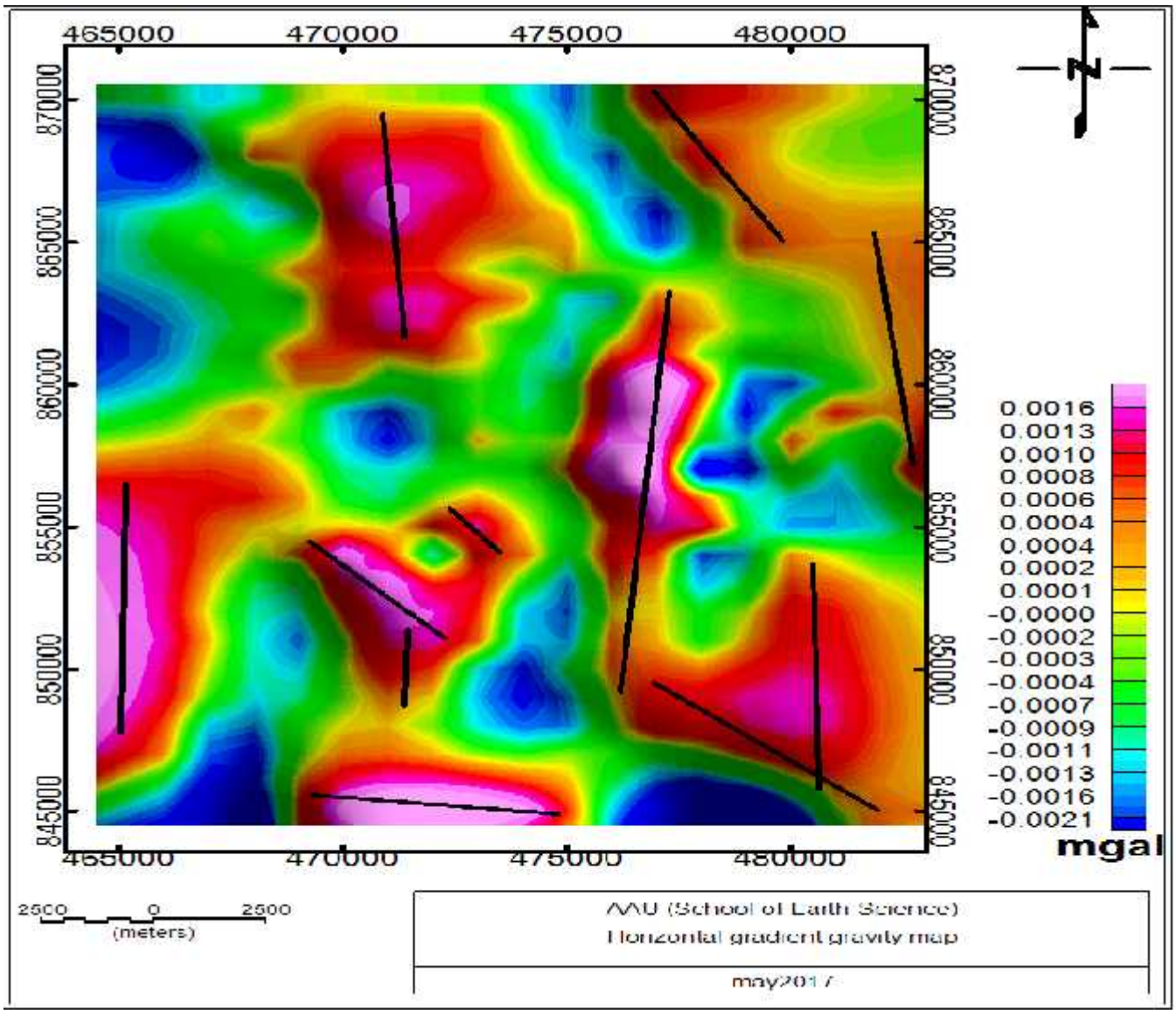

Figure 5.4 Horizontal gradient gravity map of the study area

5.1.5 Euler deconvolution gravity depth map

The Euler deconvolution gravity data enhancement method is used to estimate the depth and location of geologic sources generating gravity anomalies. The Euler deconvolution equation which is thought to operate for gravity data in 3D was developed by Reid *et al*. (1990) given by:

$$(x - x_o)\frac{\partial \Delta g}{\partial x} + (y - y_0)\frac{\partial \Delta g}{\partial y} + (z - z_0)\frac{\partial \Delta g}{\partial z} = n(\quad - g)$$

Where $(x_o, y_{0,}, z_0)$ is the position of a source (source location) whose complete Bouguer gravity anomaly is computed at (*x*, *y*, *z*), β is the regional gravity anomaly Δg_R value, and *n* is the structural index (SI), which can be defined as the rate of attenuation of the anomaly with distance. The SI must be chosen using prior knowledge of the source geometry. For example, SI = 2 for a sphere, SI = 1 for a horizontal cylinder, SI = 0 for a fault, and SI = –1 for a contact.

The Euler deconvolution method is applied to the complete Bouguer gravity data in order to estimate the depth and location of the gravity anomaly sources. Accordingly, the Euler deconvolution gravity map (Fig. 5.5) of the study area is produced for a structural Index (S I= 0.5). The structural index (SI = 0.5) is chosen based on the objective of the survey, which is mapping the lateral and depth wise variation of linear structures (faults and fractures) found in the study area.

Euler solutions obtained from the complete Bouguer gravity data show well clustering over the area of Ziway Langano Corridor. These clustering confirms the minor faults in the geologic map and infer new faults in different directions at different depths. Combining these results in one tectonic map could be giving a clear image of the subsurface structure of the area of Ziway-Langano corridor.

The Euler map (Figure 5.5) show that high clustering of the depth solutions for SI =0.5 are values associated with regions of intense faulting, fracturing and extensional activities.

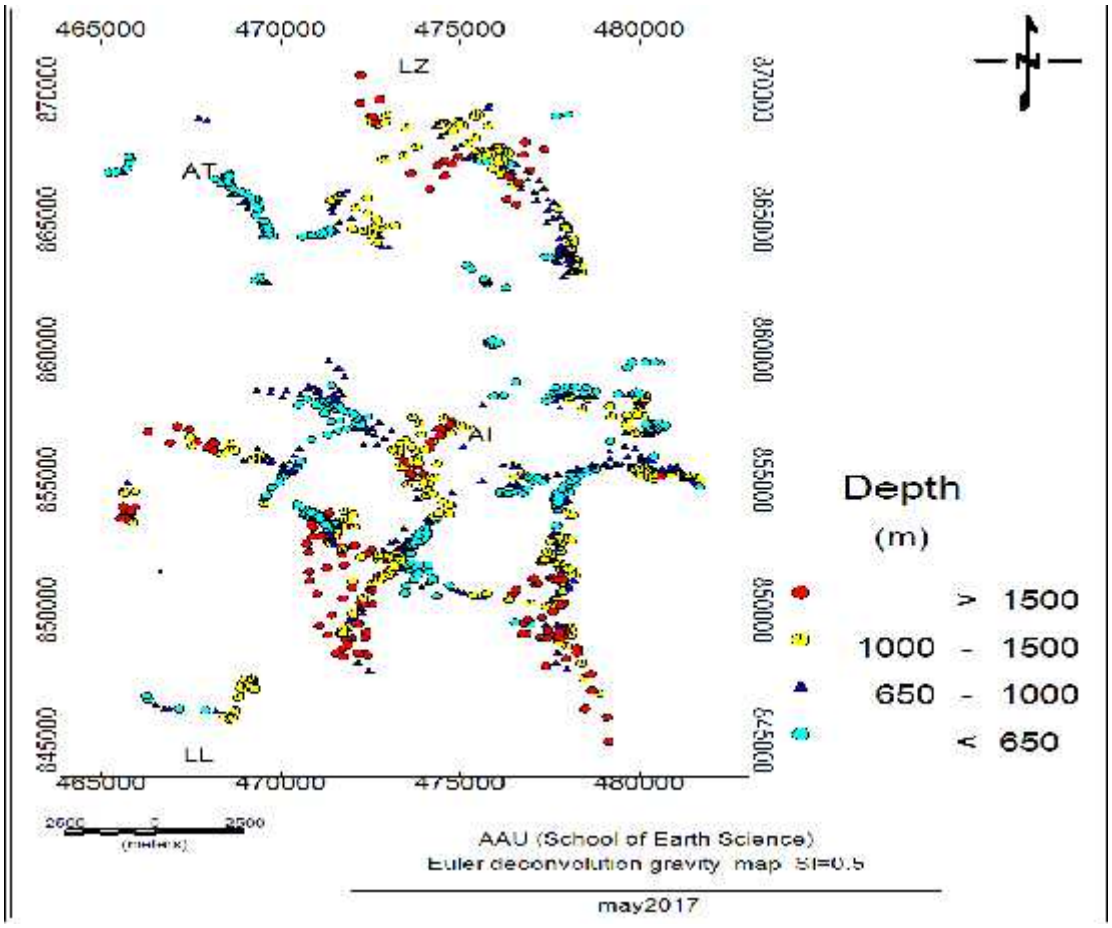

Figure 5.5 Standard Euler deconvoltion Gravity depth map for SI= 0.5

5.2 The Magnetic survey results and interpretations

The results of the magnetic survey are compiled in the form of different maps which have been generated after the field raw data have undergone through different mathematical corrections out lined in section 4.3.1 of chapter four.

It was using the IGRF corrected magnetic field anomaly values that the Total Field Magnetic Anomaly Map (TFMAM) was derived and gridded with the help of Geosoft Oasis Montaj software (V.6.4.2).

The residual magnetic field anomaly map was generated after separating the regional anomaly from the TFMAM following the use of the high pass filtering methods. Based on the residual anomaly map, different derivative maps are generated. The results of all magnetic anomaly maps included in the present work are discussed as follows:

5.2.1 Total magnetic field anomaly map

This anomaly map (Fig. 5.6), as mentioned above was generated after the field raw data have been corrected for the effects of daily and main (core) field variations in the earth's magnetic field strength during the course of data acquisition.

As can be seen from the map, high magnetic field anomalies in the range of greater than 78 Gammas characterize the eastern and NE part of the study area. Superimposed on these are, very high magnetic anomaly areas as depicted in the Central SE part of the mapped area, coinciding with the locations of the volcanic centers. The highest magnetic anomalies recorded are observed in the north and NE part of the study area associated with the Aluto volcanic complex.

The largest part of the mapped area is characterized by medium to low total field magnetic anomaly values. These include areas close to the volcanic centers of the region and located on the slopes of the volcanic centers in the North as in Aluto area volcanic centers, respectively.

Very low total magnetic anomaly values characterize the Northeastern and southern part of the study area. These areas are relatively low lands in the study area, filled with sediments and are largely covered by the lakes of the area, lakes Ziway and Langano respectively.

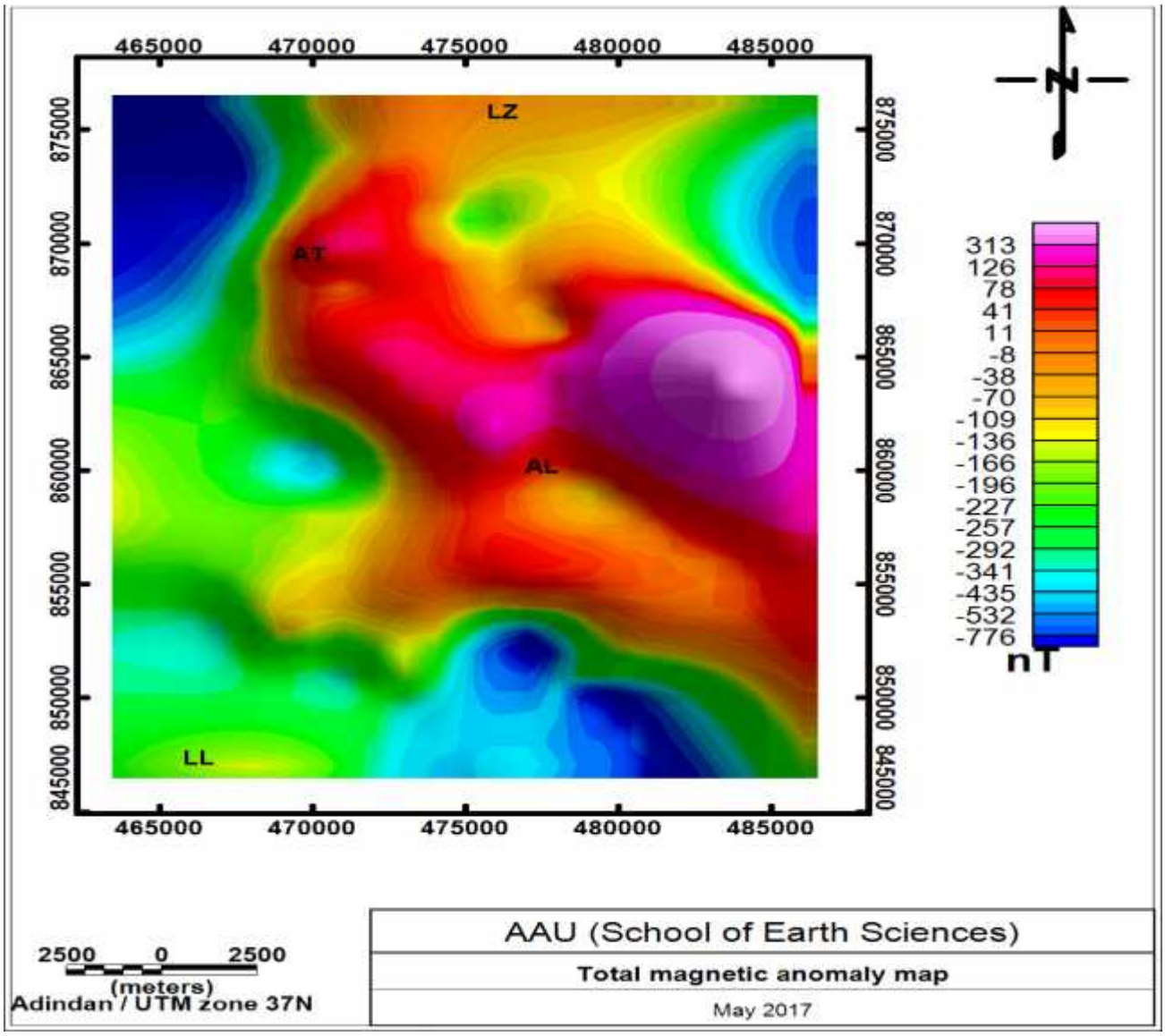

Figure 5.6 Magnetic Field Anomaly Map

5.2.2 Regional magnetic field anomaly map

The regional magnetic anomaly map of the study area was generated after low pass filtering technique has been computed using the Oasis Geosoft Montaj Soft ware (V.6.2). A general steady increase in magnetic anomalies east wards from the South/SW part of the study area, with the Northern Central Northern part being characterized by high to very high anomalies is observed in the study area. The magnetic susceptibility of geologic materials may explain the observed regional increase in the magnetic anomaly, high magnetic anomaly readings being interpreted as the responses of low magnetically susceptible earth materials, such as observed with the silicic volcanic centers of Alluto in the study area.

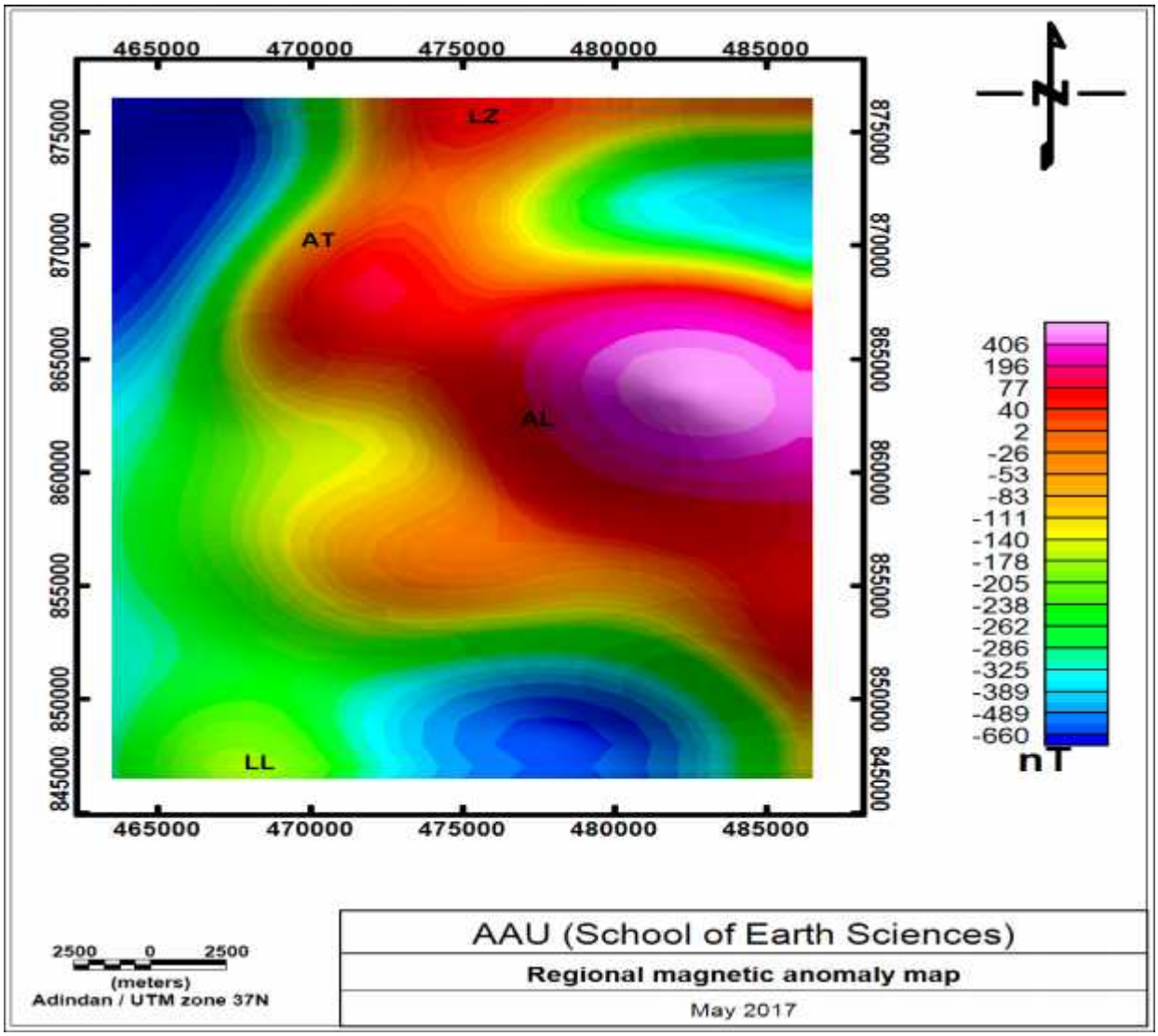

Figure 5.7 Regional magnetic field anomaly map of the study area

5.2.3 Residual magnetic field anomaly map

The residual magnetic anomaly map (5.8) was generated after the separation of the regional anomaly from the total Magnetic Field data. The map depicts subsurface features in detailed better than those revealed by the observed total magnetic field map. High to very high residual anomalies characterize to the Southern and the Northern part of the study area. Very elongated, trending approximately N - S high anomaly segment characterize the Central Western part of the mapped area. The very high residual anomalies observed in this area are in the form of mostly patches and elongated features.

As depicted in the map, the north eastern, the central and the southwestern part of the study area are characterized by low to very low magnetic anomaly values. These regions are largely occupied by the major lakes and their surroundings which are filled with Quaternary sediments.

It is determined that there exists an inverse relationship between magnetic susceptibility behavior of geologic materials and their magnetic anomaly responses in equatorial areas. As the present study area is located very close to the magnetic equator, the high magnetic anomaly observed over the volcanic complexes are associated with the low susceptibility volcanic materials that resulted from the high heat flow associated with the volcanoes. (In other words, the observed high magnetic anomalies over the volcanic complexes are due to low susceptibility materials that are magnetized by the earth's equator magnetic field).

Conversely, the observed negative anomalies could be thought to result from the relatively high susceptibility sedimentary rocks (not affected by high heat flow) derived from the neighboring volcanic complexes.

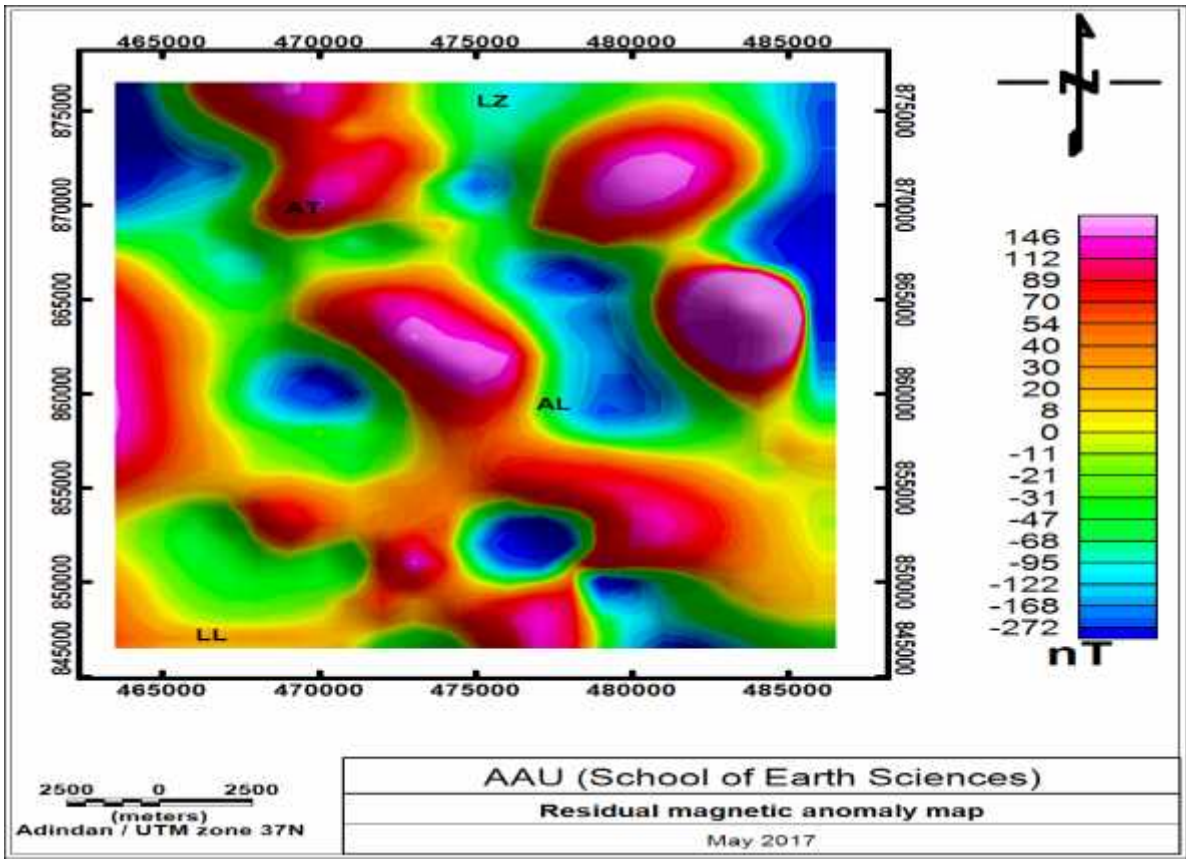

Figure 5.8 Residual magnetic field anomaly maps

5.2.4 Analytical signal (total gradient)

The Analytical signal of a potential field, such as magnetic field, is generated by combining the 3-directional gradients of the potential field at location (X,Y) in use and is given by the following formula (Dentith and Mudges, 2014).

$$AS(x,y) = \sqrt{(\frac{\partial \Delta B}{\partial x})^2 + (\frac{\partial \Delta B}{\partial y})^2 + \frac{\partial \Delta B}{\partial z})^2}$$

Where, ΔB is the residual magnetic anomaly field

The Analytical signal has the form of the ridge located above the vertical contact and is slightly displaced when the contact is dipping with the crest of the ridge delineates the edge of the top surface.

The width of a maximum or ridge is an indicator of depth of the contact, as long as the signal arising from a single contact can be resolved (GETECH Group Plc., 2007)**.**

The analytical signal map of the study area is generated after performing analytical enhancement filtering on the residual magnetic anomaly map already produced. As can be seen from the map (Fig.5.9), forms of ridges, with magnetic anomaly peaks are observed both on the NE, SW and central part of the mapped area. These observations seem to coincide with the magnetic anomaly highs identified in the residual magnetic anomaly map. These zones are also coincident with the zones where magmatic intrusions are associated with.

Accordingly, there are two evident structural contacts identified (indicated by the thick white broken lines, Fig. 5.9), with a general trend of NW- SE and NE –SW, with the majority of these structural contacts aligned in a NW – SE trend.

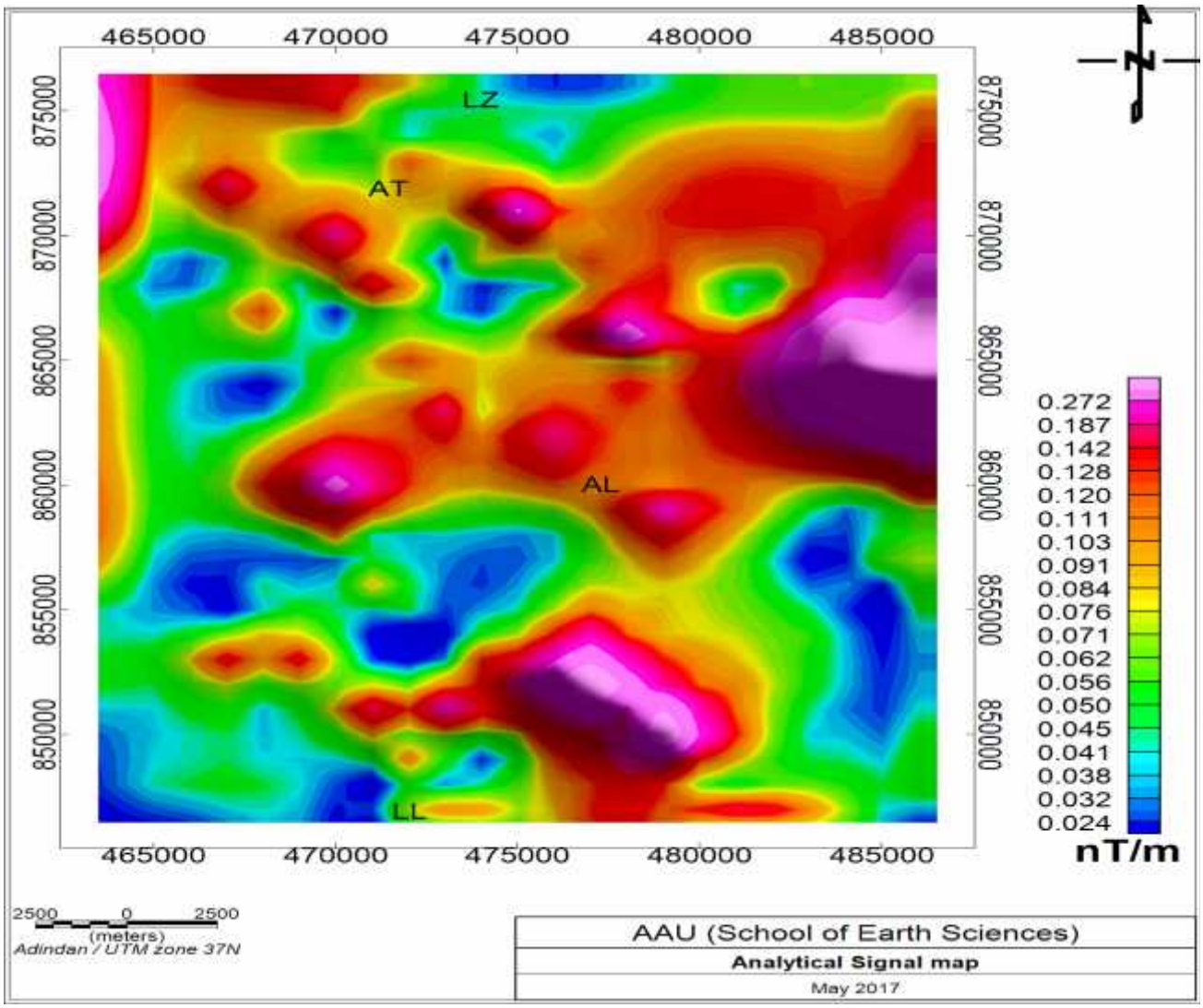

Figure 5.9 Analytical signal magnetic maps

5.2.5 Tilt derivative magnetic map

According to Miller and Singh, (1994); the Tilt Derivative maps are used to locate the edges/ boundaries of geologic structures prevailing in a given area of study. In the present work, the Tilt Derivative of the Analytical signal map is generated and the map as depicted in (Fig. 5.10), shows a more refined and detailed structural contacts/ boundaries (as delimited by the black broken lines, Fig. 5.10), than was observed in the residual magnetic anomaly map and the its counter analytical signal map.

According to the rules of interpretations of Tilt Derivative Maps, the maximum (peak) values in the map correspond to the contact or boundaries of geologic structures. As can be seen from the Tilt Derivative Map of the Analytical Signal Map generated in the present work, the study area is characterized by numerous structures delineated by contact/boundaries. The result is in good agreement with the geologically studied surface results that the study area has been subjected to extensive faulting and fracturing activities over the course of its geological history.

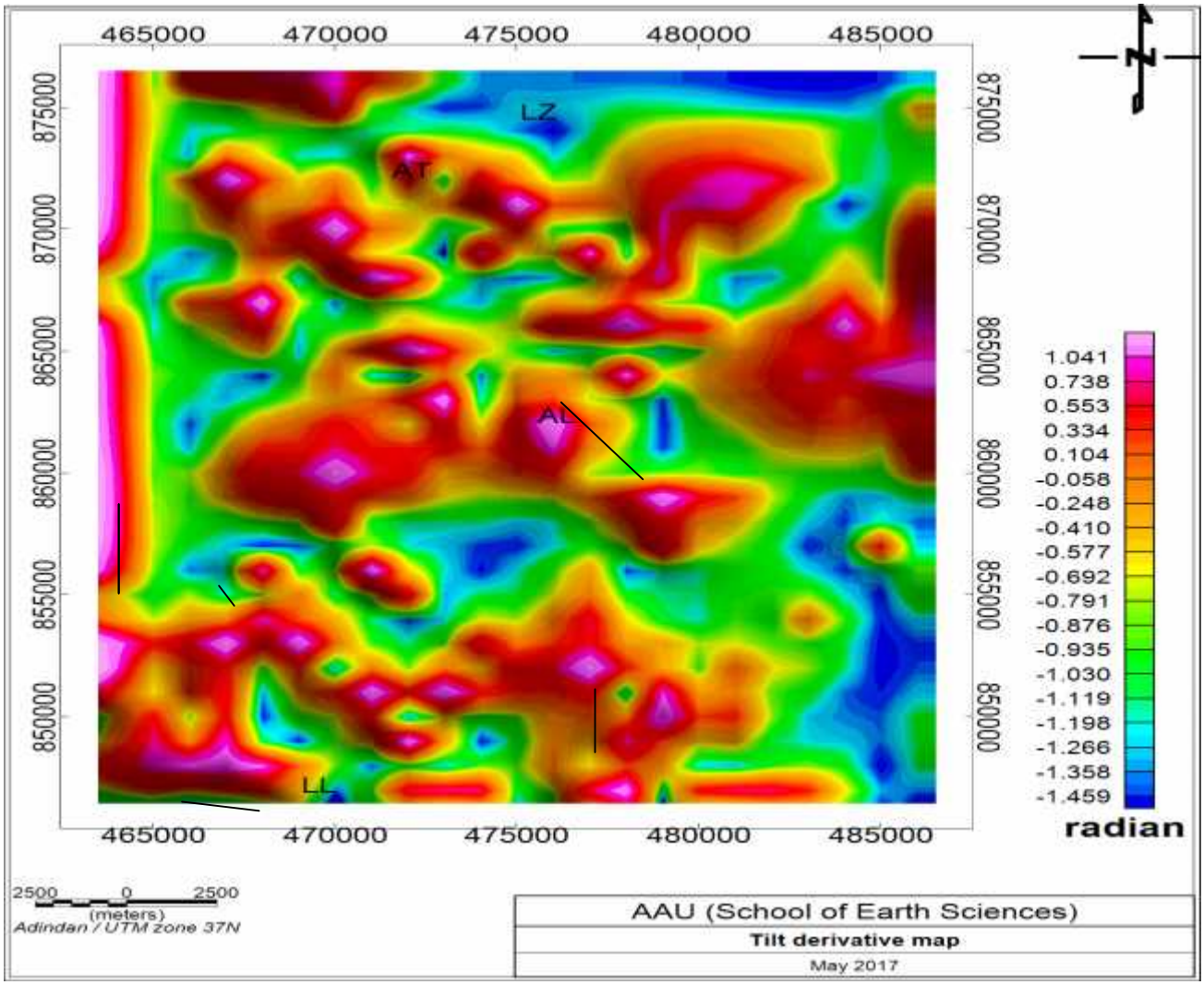

Figure 5.10 Tilt Derivative of the magnetic map

5.2.6 Euler deconvolution magnetic maps

The magnetic Euler depth maps like that of their gravity counter parts show that the prevailing geological features are located close to the surface with a depth range of less than five of kilometers.

The clustering of the depth solutions again show similar trend of locations as in the gravity Euler depth maps.

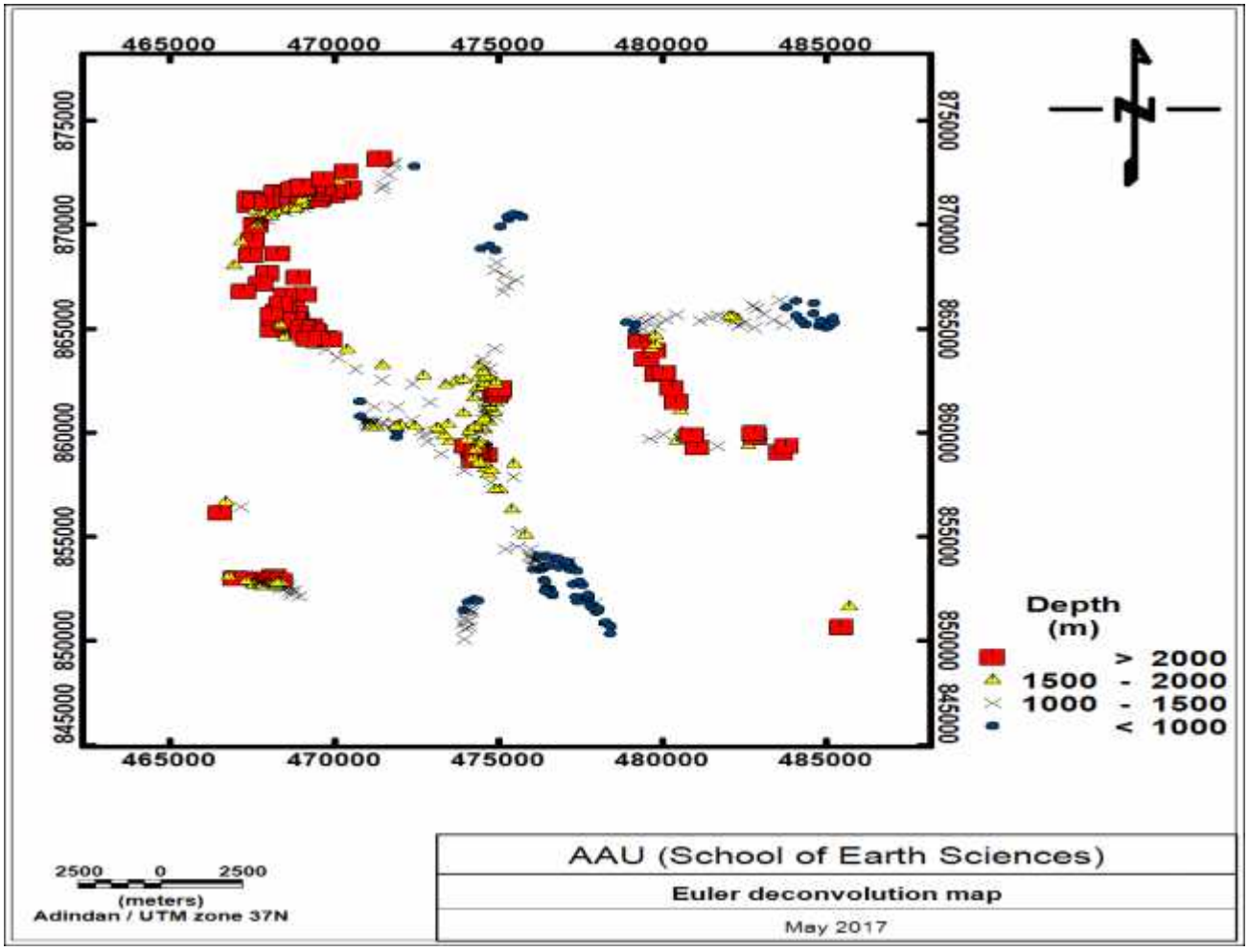

Figure 5.11 Euler deconvolution magnetic depth map for SI = 1

5.4 Combined qualitative interpretation of the gravity and magnetic survey results

In the study area, most of the high anomaly responses from the geophysical methods utilized in the present work show a close correlation in delineating the subsurface geologic structural features beneath localized zones. The observed comparatively positive anomalies largely occur at the locations of the volcanic complexes. In contrast, the observed relatively negative geophysical

anomaly responses appear to be associated with the areas that lie adjacent or away from the volcanic complexes, particularly close to the shores of Lake Ziway and Lake Langano.

In qualitative terms, the gravity highs (refer to the different gravity anomaly maps under section 5.1) and the magnetic highs (refer to the different magnetic anomaly maps under section, 5.2) considered in the study area are associated with the zones that are characterized by the volcanic centers.

The gravity highs and magnetic highs are exclusively linked with the volcanic centers of Aluto in the North/NE in the Central sections of the study area.

Interpretations of the geophysical responses vary from one method to another, as far as resource exploration, particularly subsurface structure is considered, the geophysical survey tools seeks to delineate the gravity and magnetic methods are used to delineate the subsurface structures which favor for the formation of ground water.

The gravity and magnetic highs in almost all of the maps generated (depicted under sections 5.1 and 5.2), are associated with the Aluto volcanic complex in the study area.

All the geophysical investigation results leads to the conclusion that the shallow depth subsurface structures identified beneath the study area control the ground water flow from Lake Ziway to Lake Langano.

5.5 2D Gravity modeling

To give a tentative quantitative interpretation regarding the subsurface lithological units of the study area a 2D gravity modeling was constructed along profile P1and profile P2 (Fig 5.17) in the study area.

The gravity models are prepared using the anomaly values extracted from the residual Bouguer gravity anomaly map (Fig. 5.3) also given here below. The Geosoft Oasis Montaj GM-SYS 2D gravity modeling software is used for both models.

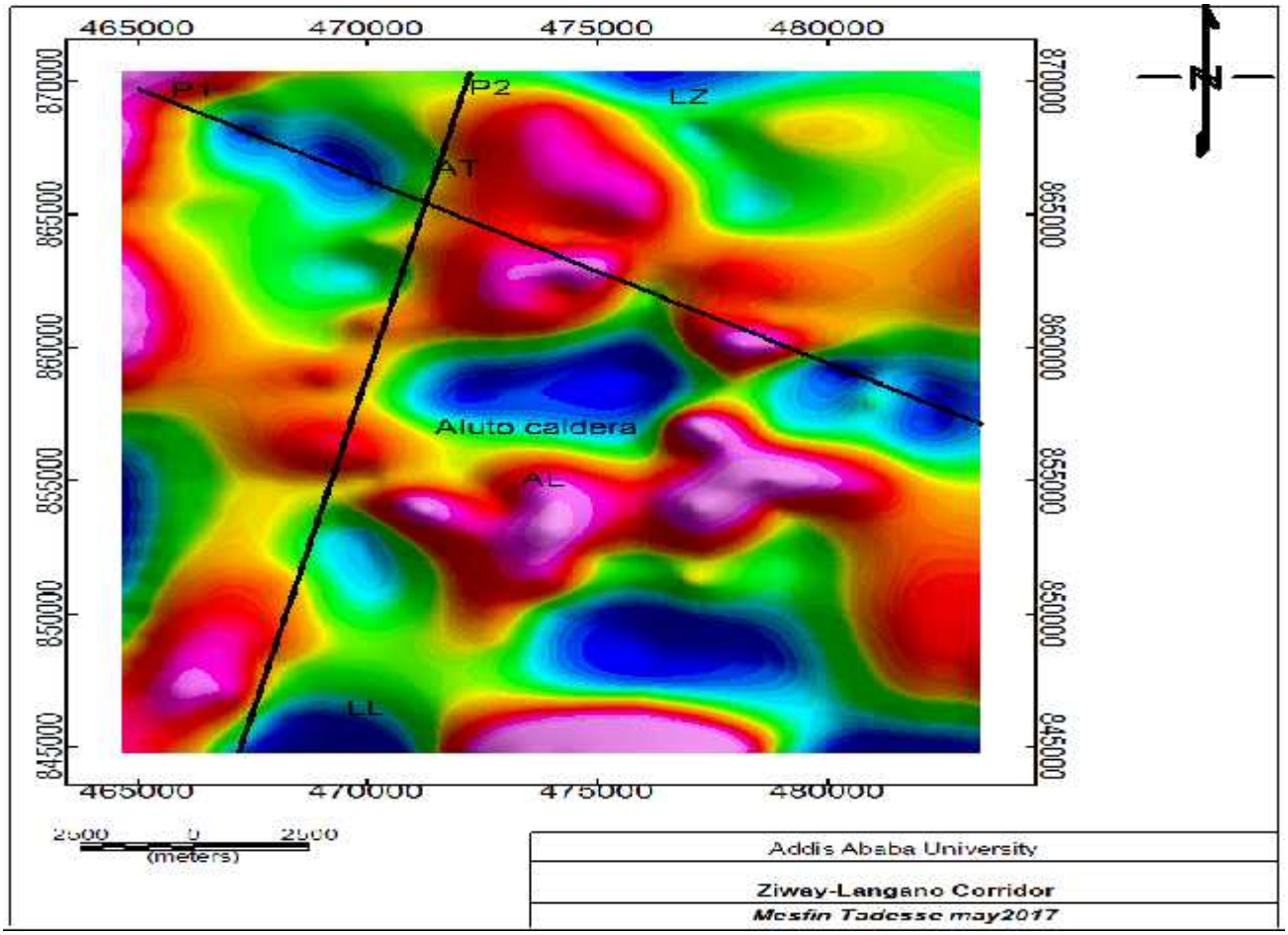

Figure 5.3 Residual gravity map

A priori density model was obtained from the work of Saibi (2012) in the Aluo geothermal system. Accordingly, the first layer consists of Quaternary volcanic products of Aluto volcano (ash flow tuffs, silicic lithic tuff breccias, silicic domes, pumice). The second layer consists of Pleistocene–Holocene lacustrine sediments with an average thickness of 400 m. The third layer includes fissural

basalt, named the Pliocene Bofa basalt; the unit has a thickness of approximately 800 to 1000 m. The fourth layer is represented by Tertiary ignimbrite (silicic unit) with a thickness of 700 m.

5.5.1 2D Gravity model along profile P1

The 2D gravity model (Fig. 5.17) is constructed along profile P1 runs in a NNE - SSW direction which is aimed to show variation in density and lithological units across the Ziway – Langano corridor.

The 2D gravity model (Fig. 5.17) constructed along profile P1consists of four layers based on the depth / lithology and density constraints considered for the initial model. A further adjustment of these parameters resulted in a fit between the observed and calculated gravity values (Fig. 5.17). The error determined for the fit between the observed and calculated gravity values is 0.163 %.

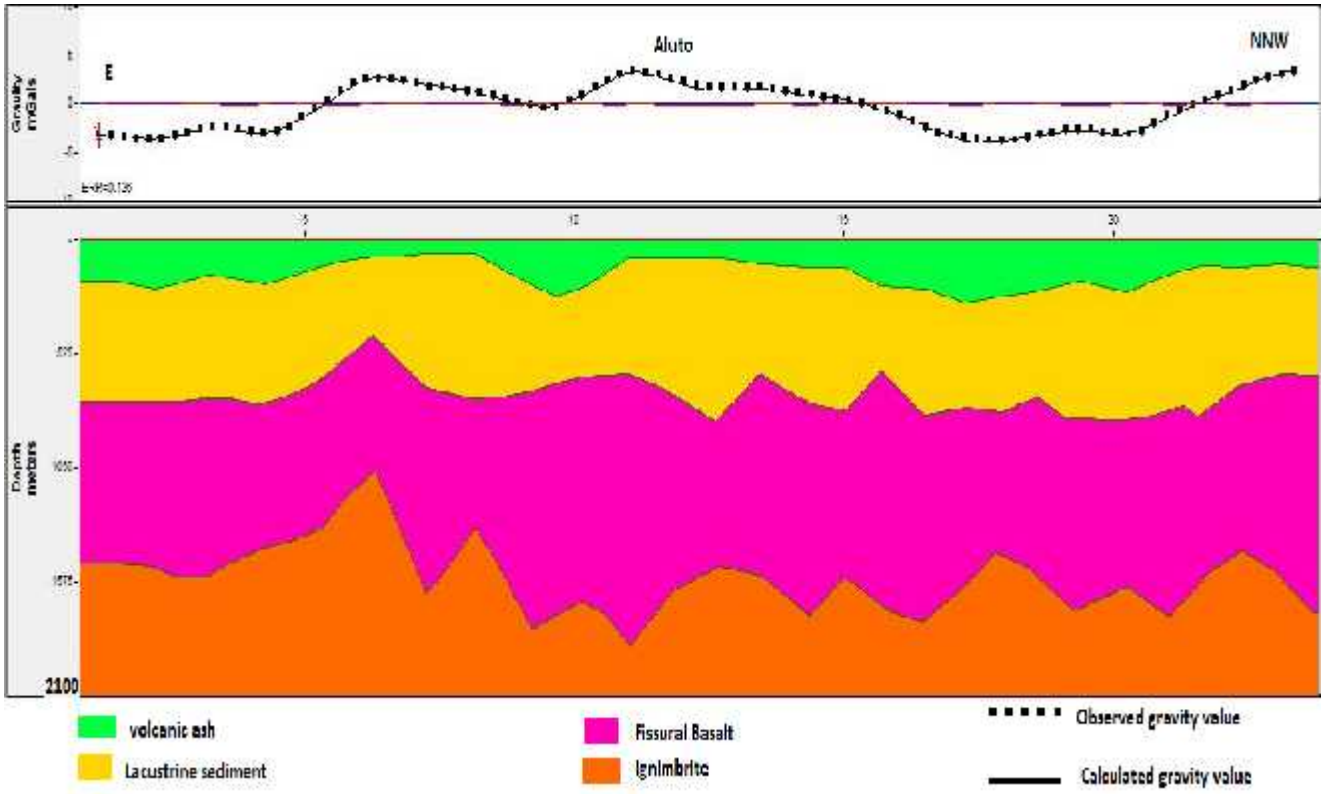

Figure 5.17 a2D Gravity modeling of the study area

The final gravity model corresponding to the first layer consists of relatively low density near surface volcanic ash products with an average density value of about 1700 kg/m^3. The average

thickness of this layer varies from 100-150 m. The second Layer has an average density value of 2180 kg/m^3 is interpreted as pleistocine – holocine lacustrine Sediment and underlain by Basalt rocks with an average thickness ranging from 400-550m. The third layer shows thick fissural Basalt at the top of Aluto and thin Basalt deposit in the Aluto caldera. The fourth layer is interpreted as ignimbrite rocks overlain by Basalt rocks with an average thickness ranging from 800-900m.

5.5.2 2D Gravity model along profile P2

The 2D gravity model (Fig. 5.18) is constructed along profile P2 runs in a north - south direction which is aimed to show variation in density and lithological units along the Ziway–Langano corridor. The model consists of four layers determined on the basis of the depth / lithology and density constraints considered for the a priori model. A further adjustment of the initial parameters resulted in a fit between the observed and calculated gravity values (Fig. 5.18). The error determined for the fit between the observed and calculated gravity values is 0.127 %.

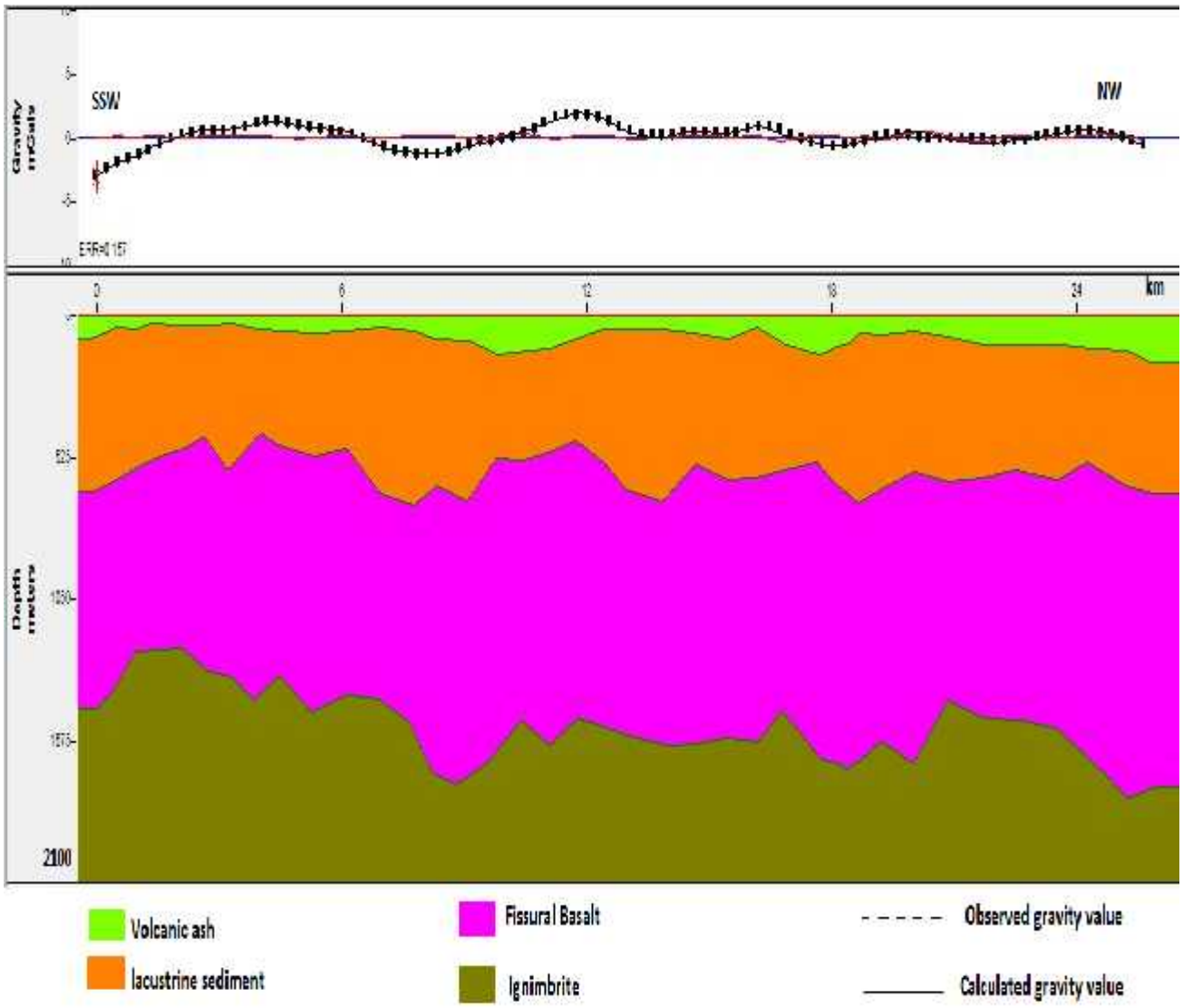

Figure 5.18 2D Gravity modeling of the study area

The final gravity model corresponding to the first layer consists of relatively low density near surface volcanic ash products with an average density value of about 1700 kg/m^3 .The average thickness of this layer varies from 100-150 m. The second Layer has an average density value of 2180 kg/m is interpreted as pleistocine – holocine lacustrine Sediment and underlain by Basalt rocks with an average thickness ranging from 400-550m. The third layer shows thick fissural Basalt at the top of Aluto and thin Basalt deposit in the Aluto caldera. The fourth layer is interpreted as ignimbrite rocks overlain by Basalt rocks with an average thickness ranging from 800-900m.

The conclusion drawn based on a preliminary interpretation of the 2D gravity models is that:

1. Beneath the top of the Aluto volcanic complex, the thickness of low density volcanic ash (layer 1) deposit varies from 50-100m and the thickness of the lacustrine sediments (layer 2) ranges from 450-500m. The thickness of the fissural basalt (layer 3) ranges from 600-650m and the thickness of ignimbrite rock units (layer 4) are estimated to about 900m.
2. Beneath the centrer of the Aluto complex (Aluto caldera) the thickness (about 200m) of low density volcanic ashes (layer 1) are thicker as compared to those residing the top parts of the volcano (Aluo ridge). The thickness of the Pleistocine - Holocine lacustrine sediments (layer 2) ranges from 450-500m, thickness of the fissural basaltic rock (layer 3) deposit is estimated to about 500-550m and the thickness of ignimbrite rock (layer 4) is estimated to about 900m.
3. Beneath the Lake Ziway and Lake Langano thickness of the volcanic ash products (layer 1) ranges from 50-150m. The thickness of the Pleistocine – Holocine lacustrine sediments (layer 2) ranges from 450-650m, thickness of the fissural basalt (layer 3) in these areas are estimated to about 450-550m and the thickness of ignimbrite rock (layer 4) deposit is estimated to about 900-1050m.

Investigation results based on the 2D gravity models indicate that the subsurface rock units in the study area constitute volcanic ash, lacustrine sediment, basalt and ignimbrite rocks. The depth range of these rock units ranges from surface to 2100 m. Furthermore, the relatively high porosity and permeability of these rock units is thought to allow the flow of groundwater from Lake Ziway towards Lake Langano.

5.6. 2D Magnetic model along profile P1

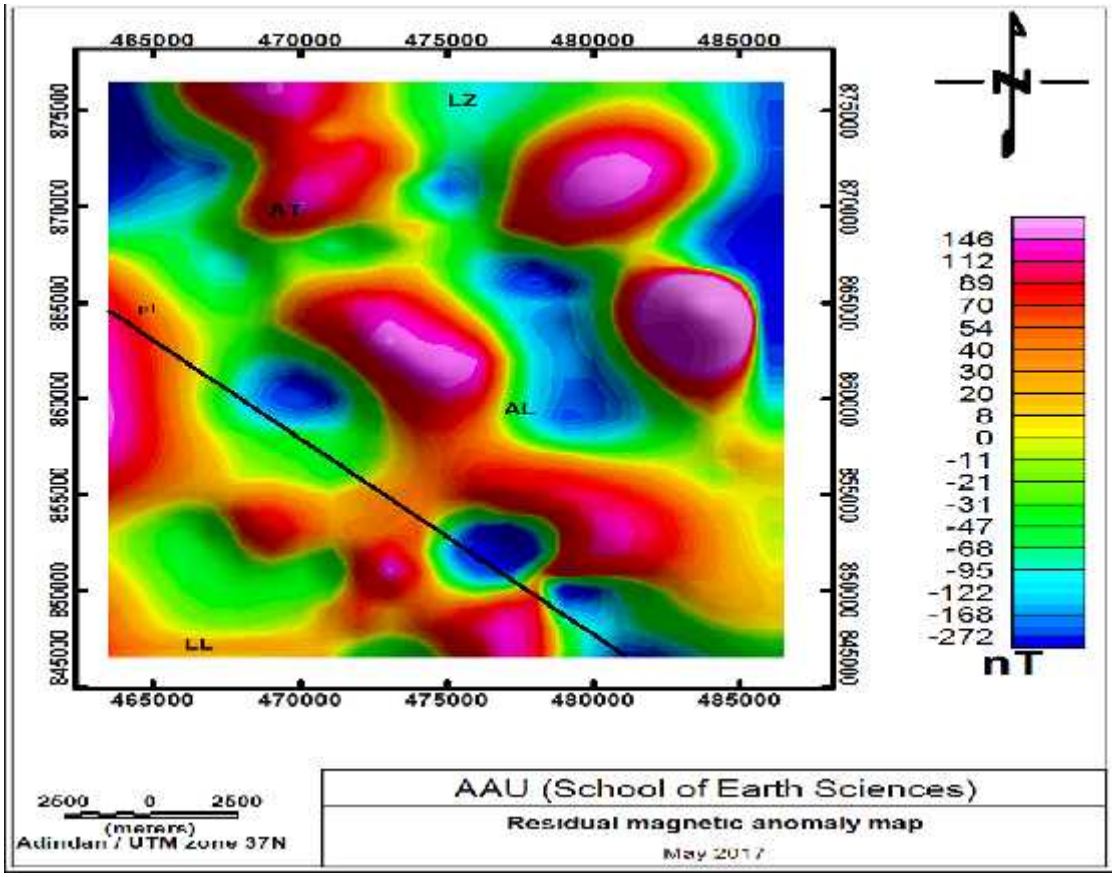

Figure 5.19 Residual magnetic anomaly map

The 2D magnetic model is constructed using the GM-SYS modeling software. Any difference between the model response and the observed magnetic field are reduced by refining the model structure. It should be noted that magnetic models are non unique, i.e. many earth models can produce the same magnetic response, and similarly, several geological lithologies may be interpreted from a given model block's susceptibility properties. It is therefore important to use as many independent source of information as possible to constrain a model.

The magnetic model corresponding to the first layer consists of relatively low sucessptibility near surface volcanic ash products with an average successptibility value of about 0.0012cgs

The average thickness of this layer varies from 150-250 m. The second Layer has an average magnetic sucessptibilty value of 0.0186 is interpreted as pleistocine – holocine lacustrine Sediment

and underlain by Basalt rocks with an average thickness ranging from 550-650m. The third layer shows thick fissural Basalt at the top of Aluto and thin Basalt deposit in the Aluto caldera. The fourth layer is interpreted as ignimbrite rocks overlain by Basalt rocks with an average thickness ranging from 700-800 m.

Accordingly 2D magnetic modeling is developed along profile-1 from the residual magnetic map as shown in Figure 5.19. The developed model has an error of 1.26nT.

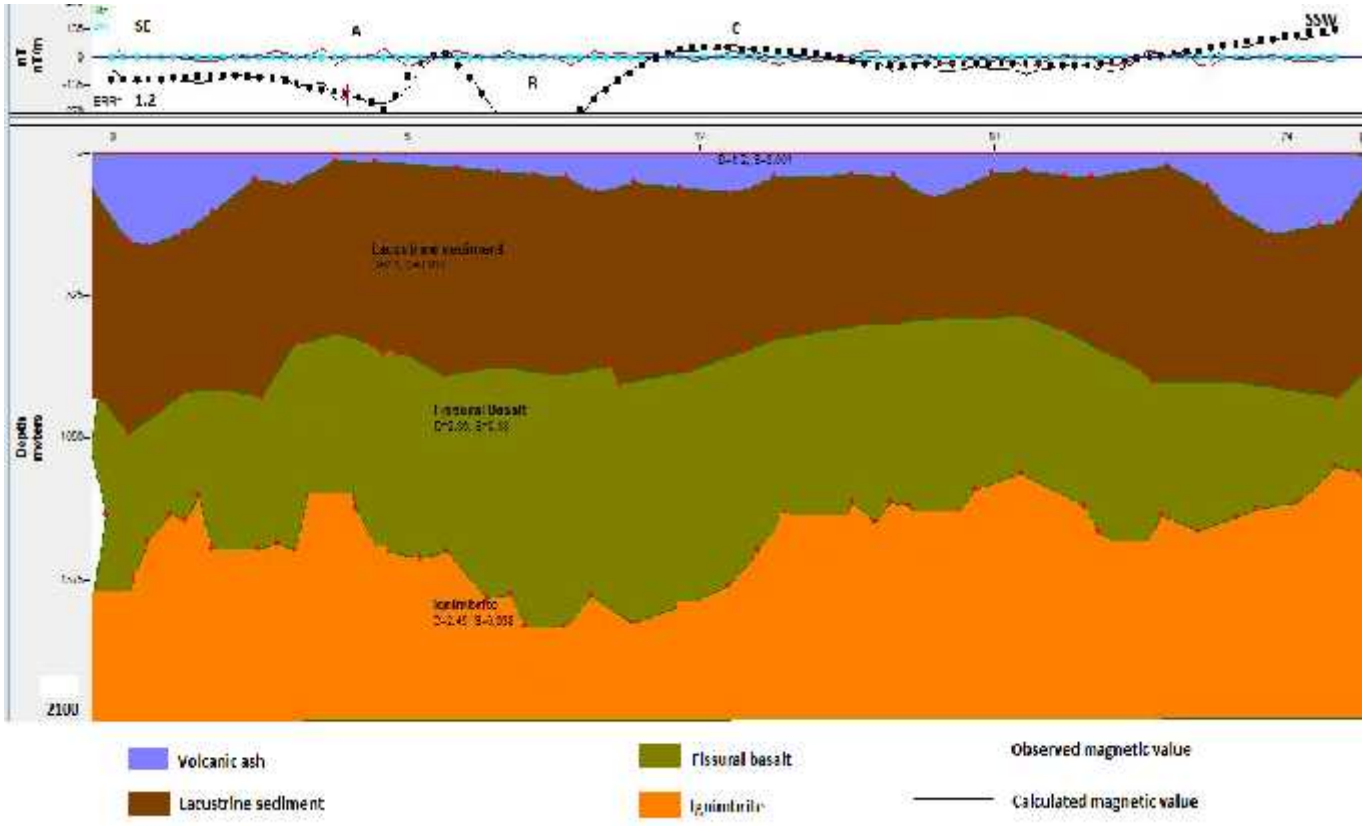

Figure 5.20 2D Magnetic modeling of the study area

CHAPTER SIX

6.0 CONCLUSIONS AND RECOMMENDATIONS

6.1 Conclusions

Considering the magnetic and Gravity areas of low magnetic and Gravity anomaly (with surface manifestations and alterations) are mapped. These areas of low geophysical anomalies are interpreted to be highly water saturated region due to the close proximity of the observed profiles to the Langano and Ziway lakes.

Lowering of gravity and magnetic susceptibility could suggest the circulation of ground water through the fractures/faults to result in ground water flow.

The N-S and NNE - SSW trending linear subsurface features (faults and fractures) revealed by both the horizontal gradient gravity map and tilt derivative Magnetic map are considered to be the major geologic structures that favor the flow of ground water from Lake Ziway towards Lake Langano.

6.2 Recommendations

Based on the outcome of this study, the following are recommended

- ✓ It is recommended that to study detailed structural geological investigations for mapping the orientation of lineaments,
- ✓ Additional resistivity and magnetic survey data is recommended
- ✓ Integrating all the geophysical results to hydro geological, geological and structural geology of the study area is important for a detailed investigation of the subsurface structure and groundwater flow of the area.

References

Abera, A. (1992). The Gravity Field and Crustal Structure of the Main Ethiopian Rift. Report No. 26. TRITA GEOD 1026. Stockholm, Sweden.

Bekele Abebe, Acocella, V., Tesfaye Korme and Dereje Ayalew (2007). Quaternary faulting and volcanism in the Main Ethiopian Rift. J. Afr. Earth Sci. **48**: 115–124.

Bonini, M., Corti, G., Innocenti, F., Manetti, P., Mazzarini, F., Tsegaye, A. and Pecskay Z. (2005). Evolution of the Main Ethiopian Rift in the frame of Afar and Kenya rifts propagation. Tectonics. **24:** TC1007, doi: 10.1029/2004TC001680.

Corti, G. (2008). Control of Rift Obliquity on the evolution and Segmentation of the Main Ethiopian Rift. Letters. Doi: 10.1038/ngeo160.

Corti, G. (2009). Continental Rift evolution: From rift initiation to incipient break-up in the Main Ethiopian Rift, East Africa. Earth Science Reviews. **96:** 1 – 53.

Dentith, M. and Mudge, S.T. (2014). Geophysics for the Mineral exploration Geoscientist. Cambridge University Press, New York, USA.

Di Paola, G.M. (1972). The Ethiopian Rift Valley (between 7° 00’ and 8° 40’ lat. North). Bull. Volcano: **36:** 517 - 560

Di Paola, G.M., Seife, M.B., Arno, V. (1993). The Kella horst: Its origin and significance in crustal attenuation and magmatic processes in the Ethiopian Rift Valley. **In:** Geology and Mineral Resources of Somalia and Surrounding Regions, Ist. Agronom. Oltremare, Firenze, Relaz. Monograph. **113:** 323 – 338.

Dobrin, M.B. and Savit, C.H. (1988). Introduction to Geophysical Prospecting. McGraw. Hill Inc. Singapore.

Ebinger, C.J., Yemane, T., Giday, W., Aronson, J. L. and Walter, R.C. (1993). Late Eocene – Recent Volcanism in the Southern Main Ethiopian Rift. Journal of the Geological Society, London. **150:** 99 – 108

Ebinger, C. J., Yemane, T., Harding, D. J., Tesfaye, S., Kelley, S. S. and Rex, D. C. (2000). Rift deflection, migration, and propagation: Linkage of the Ethiopian and Eastern rift. Africa, Geol. Soc. Am. Bull. **112:** 163–176.

Everett, M.E. (2013). Near Surface applied Geophysics. Cambridge University Press. United States of America. New York.

GETECH Group plc. (2007). Advanced processing and Interpretation of gravity and magnetic data.

Girdler, R.W, Fairhead, J.D, Searle, R.C. and Sowerbutts, W.T.C. (1969). The evolution of Rifting in Africa. Nature. **224:** 1178 – 1182

Girdler, R.W. and Hall, S.A. (1972). An Aeromagnetic survey of the Afar triangle of Ethiopia. **In:** R.W. Girdler (Editor), East African Rifts. Tectonophysics. **15(1/2):** 53

Gouin, P. and Mohr, P.A (1964). Gravity Traverses in Ethiopia (First Interim Report). Bull. Geophys. Obs. Addis Ababa. **7:** 185 – 239.

Hayward, N. J. and Ebinger, C. J. (1996). Variations in the along-axis segmentation of the Afar Rift system, Tectonics. **15:** 244 – 257.

Hinze, W.J., VonFrese, R.B. and Saad, A.H. (2013). Gravity and Magnetic Exploration: Principles, Practices, and Applications. Cambridge University Press, New York, USA.

Kazmin, V., Seife Michael Berhe, Nicoletti, M. and Petrucciani, C. (1980). Evolution of the northern part of the Ethiopian Rift. Accad. Naz. Lincei, Rome, **47**: 275–291.

Kearey, P., Brooks, M. and Hill, I. (2002). An introduction to Geophysical Exploration. Third edition. Black Well Science Ltd, Oxford, UK.

Keranen, K. and Klemperer, S.L. (2008). Discontinous and diachronous evolution of the Main Ethiopian Rift: Implications for development of continental rifts. Earth and Planetary Science Letters. **265:** 96- 111

Lillie, R. J. (1999). Whole Earth Geophysics: An Introduction text to geologists and geophysicists. Prentice-Hall, Inc. Upper Saddle River, New Jersey, USA

Mackenzie, G.H, Thybo, G.H. and Maguire, P. (2005). Crustal velocity structure across the Main Ethiopian Rift: Results from 2-dimenional wide-angle seismic modeling. Geophysical Journal International. **162:** 994 –1006

Meseret, T. (1996). Water – Rock interaction processes in the Aluto – Langano Geothermal Field. PhD. Dissertation. University of Pisa, Department of Earth Sciences, Italy.

Milsom, J. (2003). Field Geophysics: The Geophysical Guide Field Series. Third edition. John Wiley and Sons Ltd. West Sussex, England.

Milsom, J. and Eriksen, A. (2011). Field Geophysics. Fourth edition. John Wiley and Sons Ltd. West Sussex, UK.

Mohr, P. A. (1967). The Ethiopian Rift System. Bulletin of the Geophysical Observatory of Addis Ababa. **11:** 1-65

Mohr, P. A. (1971). The Geology of Ethiopia, University College of Addis Ababa press. Addis Ababa, Ethiopia.

Mohr, P.A. (1983). Volcanotectonic aspects of the Ethiopian Rift evolution. Bull. Cent. Rech. Explor. Prod. Elf – Aquitaine. **7:** 175–189.

Mussett, A.E and Khan, M.A (2000). Looking in to the Earth: An introduction to Geological Geophysics. Cambridge University Press, USA.

Reynolds, (1997). An Introduction to Applied and Environmental Geophysics. John Wiley and Sons Ltd. Baffins Lane, Chichester, West Sussex, England.

Revees, V.C. (1991). Potential field data processing and Interpretation. First edition. International Institute for Aerospace Survey and Earth Sciences. Delft, the Netherlands.

Rezene, M., Jentzsch, G. and Jahr, T. (1999). Crustal Structure of the Main Ethiopian Rift from gravity data: 3-Dimensional modeling. Tectonophysics. **313:** 363 – 382

Saibi et,al (2012), Analysis and Interpretation of Gravity Data from the Aluto-Langano Geothermal Field of Ethiopia

Searle, R. and Gouin, P. (1972). A gravity Survey of the central part of Ethiopian Rift. **In:** R.W. Girdler (Editor), East African Rifts. Tectonophysics, **15(1/2):** 41 -52

Solomon, K., Tadesse, M. and Tsegaye, A. (1984). Geological Report: Explanations to the Geological map of Aluto – Langano Geothermal area. Ethiopian Institute of Geological Survey.

Tadiwos Chernet, Hart, W. K., Aronson, J. L. and Walter, R. C. (1998). New age constraints on the timing of volcanism and tectonism in the northern main Ethiopian rift–southern Afar transition zone, Ethiopia. Journal of Volcanology and Geothermal Research, **80(3):** 267280.

Telford, W.M., Geldart, L.P. and Sheriff, R.E. (1990). Applied Geophysics. Second edition. Cambridge University Press. New York, USA.

Tibebu Ayele (2001) Geophysical studies in the Aluto geothermal area, MSc thesis. Addis Abeba University.

Tiberi, C., Ebinger, C., Ballu, V., Stuart, G. and Befekadu, O. (2005). Inverse models of gravity data from the Red Sea- East African rift triple junction zone. Geophysical Journal International. **163:** 775 – 787

Tsegaye, A. (2000). Geological Limitations of a Geothermal System in a continental Rift zone: Example the Ethiopian Rift Valley. **In:** Proceedings World Geothermal Congress. May 28 - June 10, Kyushu- Tohoku, Japan.

W/Gabriel Giday, Aronson, J.L., and Walter R.C., (1990). Geology, Geochronology and Rift Basin Development in the Central Sector of the Main Ethiopian Rift ,Geological Society of America, bulletin ; **102**:439-458.

Yemane K. (2016) MSc thesis. Integrated geophysical investigations of the central main Ethiopian rift and adjacent plateaus: an implication to crustal structure and Moho depth determinations